

ADAPTIVE OVER-CURRENT PROTECTION OF SPV INTEGRATED DISTRIBUTION SYSTEMS

A THESIS

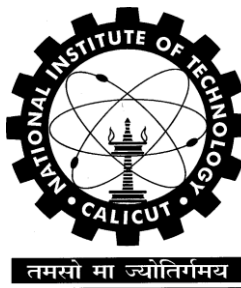
Submitted By

**OWAIS MANZOOR MALLA
(Roll No. M210473EE)**

In partial fulfillment for the award of the Degree of
**MASTER OF TECHNOLOGY
IN
ELECTRICAL ENGINEERING
(POWER SYSTEMS)**

Under the guidance of

Dr. Deepak M



**DEPARTMENT OF ELECTRICAL ENGINEERING
NATIONAL INSTITUTE OF TECHNOLOGY CALICUT**

NIT CAMPUS P.O., CALICUT - 673601, INDIA

JULY 2023

ACKNOWLEDGEMENT

First and foremost, I thank God Almighty for his blessings, which were with me throughout my work.

I would like to express my profound sense of gratitude to my project guide, **Dr. Deepak M**, Assistant Professor, Department of Electrical Engineering, for providing necessary information and guidance during the course of this ongoing work. I also express my gratitude to the Project Evaluation Chair **Dr. GOPAKUMAR P**, Assistant Professor, Department of Electrical Engineering, National Institute of Technology Calicut for the guidance provided throughout the entire process behind this work. It was they who encouraged me to tackle all the difficulties I faced during the work.

I use this opportunity to thank **Prof. PREETHA P**, Professor and Head, Department of Electrical Engineering, for providing me with the best facilities for the completion and presentation of my Main project dissertation.

I would like to thank the National Institute of Technology Calicut for providing me with sufficient infrastructure and technical support in this project.

Finally, yet importantly, I would like to express my heartfelt thanks to my beloved parents and brothers for their blessings and support during all difficulties in the work, I also extend my sincere gratitude to my friends and classmates for their help and wishes for the successful completion of this dissertation.

OWAIS MANZOOR MALLA

DECLARATION

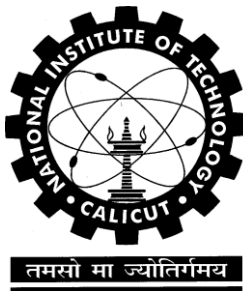
I hereby declare that this submission is my own work and that, to the best of my knowledge and belief, it contains no material previously published or written by another person nor material which has been accepted for the award of any other degree or diploma of the university or other institute of higher learning, except where due acknowledgment has been made by me in the text.

Place: Calicut

Name: OWAIS MANZOOR MALLA

Date: 04/07/2022

Roll No: M210473EE



CERTIFICATE

*This is to certify that the thesis entitled “ADAPTIVE OVER-CURRENT PROTECTION OF SPV INTEGRATED DISTRIBUTION SYSTEMS” submitted by **Mr. OWAIS MANZOOR MALLA** (Roll No.M210473EE) to the National Institute of Technology Calicut towards partial fulfillment of the requirements for the award of **Degree of Master of Technology in Electrical Engineering (Power Systems)** is a bona fide record of the work carried out by him, under my supervision and guidance.*

Dr Deepak M
(Guide)
Asst. Professor
Dept. of Electrical Engineering

Attested by

Dr Preetha P
Professor & Head
Dept. of Electrical Engineering

Place: Calicut
Date: 04/07/2023

Abstract

As the integration of solar photovoltaic (SPV) with traditional grid systems increases, various protection issues in distribution systems arise because of modified network topologies, limited fault current contribution, and bidirectional power flow. The low fault current contribution of inverter-based resources due to the thermal constraints of inverter switches causes the malfunction of the conventional over-current relay in the distribution system. In this project work, the penetration of PV into the grid is about 25% concerning the load. PV-plant can operate in different modes of operation. In this project, the PV plant is operated in voltage control mode. In this mode of operation, the PV plant complies with Grid Codes i.e., follows the Fault ride-through condition. The PV system supports the voltage at the fault bus by supplying reactive power during a fault. An adaptive over-current relaying method is developed for the protection of a high-penetration PV integrated grid. The positive sequence current and voltage component is being utilised for the detection of faults and the same is tested on an IEEE 9-bus system. The outcomes are accurate. The method is developed using PSCAD software.

Keywords - Distribution Systems (DSs), Fault Ride Through (FRT), Over-Current Relay (OCR), Positive Sequence Component, Reactive Power, Solar Photo Voltaic (SPV).

CONTENTS

List of Figures	iii
List of Tables	v
Abbreviations	vi
List of symbols	vii
1 INTRODUCTION	1
1.1 Introduction	1
1.2 Background	1
1.3 Motivation	2
1.4 Literature Survey	2
1.5 Objectives	3
1.6 Outline of Report	4
2 Solar Photo Voltaic system Modelling	5
2.1 Introduction	5
2.2 Power Plant Controller	6
2.3 SPV module Setup	6
2.4 Controller units and circuit layout of solar farm	8
2.4.1 SPV Boost Converter	8
2.4.2 Voltage Source Converter	8
2.4.3 PLL and ABC-to-DQ0 Transformation	12
2.5 Fault Ride-Through (FRT)	15
2.6 Summary	15
3 Fault Analysis of Grid Integrated Photo Voltaic	17
3.1 Introduction	17
3.2 PV-Integrated Grid	17
3.3 Fault Characteristics of Inverter-based DER	18
3.4 Inverter Operation Under Fault Conditions	19
3.4.1 Symmetrical Fault (LLLG)	19

3.5	Summary	20
4	Overcurrent Protection of distribution systems	21
4.1	Over-Current Protection	21
4.2	Extremely Inverse Over-current Relay	22
4.2.1	Fault Detection	23
4.3	Voltage-restrained Over-current Relay	24
4.3.1	Effect of loading percentage on relay current	25
4.4	Summary	26
5	Simulation Results and Discussion	27
5.1	Introduction	27
5.2	Over-Current Fault Simulation results	30
5.2.1	Line to Ground fault	30
5.2.2	Line to Line to Line fault(LLL)	31
5.3	Voltage-Restrained Over-Current	31
5.3.1	Line to Ground Fault	32
5.3.2	Line to Line to Ground Fault	32
5.3.3	Line to Line to Line to Ground Fault	32
5.4	VR-OCR with different loading conditions	36
5.4.1	At 50% loading condition	38
5.4.2	At 100% loading condition	40
5.5	Summary	41
6	Real Time implementation of PV-Integrated Grid	42
6.1	Introduction	42
6.2	Speedgoat Target Machine	42
6.3	Implementation of PV-integrated grid into Speedgoat	43
6.3.1	MATLAB model with voltage restrained OCR	43
6.3.2	Real Time implementation	44
6.4	Summary	45
7	Conclusion and Future Work	47
7.0.1	Conclusion	47
7.0.2	Future Work	47
APPENDIX		49
Publications		51
REFERENCES		52

List of figures

2.1	Solar farm integrated with power system grid	6
2.2	Power plant controller	6
2.3	Input parameters of PPC	7
2.4	Circuit configuration for measuring Open circuit voltage , short circuit current and maximum power of SPV module	7
2.5	Variation of resistance with simulation time	8
2.6	Variation of SPV parameters as a function of resistance variation	9
2.7	Configuration of SPV array	9
2.8	Overall Solar farm module	9
2.9	Solar Farm input parameters	10
2.10	Boost converter connected to SPV array	10
2.11	Boost controllers	11
2.12	PV module consisting of PV array, Booster converter, VSC, LCL Filter, and Damper respectively	11
2.13	Phase Lock Loop and the ABC-to-dq transformation	12
2.14	Outer controllers	13
2.15	Frequency droop characteristic and the dead band controller	13
2.16	d- and q-frames current limit calculation	14
2.17	Inner current controllers and decoupled components	14
2.18	Reference voltages provided by grid-side controller	15
3.1	Active power and Reactive power supply by PV in nominal condition	18
3.2	Per unit voltage and current supplied by PV during nominal condition	19
4.1	Characteristics of inverse-time-over-current relay	22
4.2	Simple 9-Bus system with LG fault at bus-2	23
4.3	Shows the relay logic of OCR and breaker status circuit	24
4.4	Conventional tripping characteristics of VR-OCR	25
4.5	Shows the relay logic of VR-OCR and breaker status circuit	25
4.6	A PV plant integrated 4-bus distribution system	26
5.1	Fault at POC of SPV at 5 sec of time	27
5.2	Voltage dip at POC bus in pu during fault	27

5.3	supply of reactive power in pu after the inception of fault	28
5.4	Fault current supplied by SPV in pu	28
5.5	SCC in its sequence representation for a LLLG:(a) grid contribution and (b) PV inverter contribution	29
5.6	SCC in its sequence representation for an SLG: (a) grid contribution and (b) PV inverter contribution	29
5.7	SCC in its sequence representation for an LLG fault event	30
5.8	A PV plant integrated three-bus distribution system	30
5.9	CT primary and secondary fault level and positive sequence current of LG fault	31
5.10	CT primary and secondary fault level and positive sequence current of LLL fault	31
5.11	A PV plant integrated 4-bus distribution system	32
5.12	RMS current of LG fault	33
5.13	RMS voltage of LG fault	33
5.14	Pick-up current of LG fault	34
5.15	RMS current of LLG fault	34
5.16	RMS voltage of LLG fault	35
5.17	Pick-up current of LLG fault	35
5.18	RMS current of LLLG fault	36
5.19	RMS voltage of LLLG fault	36
5.20	Pick-up current of LLLG fault	37
5.21	Voltage and current seen by relay for different faults	37
5.22	Voltage and current seen by VR-OCR during fault at 0%, 50% and 100% loading condition .	38
5.23	Schematic diagram of PV integrated 4-Bus system	39
5.24	Proposed adaptive VR-OCR characteristics for 50% loading conditions at PV bus	39
5.25	Proposed adaptive VR-OCR characteristics for 100% loading conditions at PV bus	40
5.26	Existing and Proposed adaptive VR-OCR characteristics for different loading conditions at PV bus	40
6.1	Speedgoat hardware module	43
6.2	MATLAB 3-bus model	43
6.3	Fault current after the opening of circuit breaker	44
6.4	Open circuit voltage during fault	45
6.5	Open circuit voltage during fault	45

List of Tables

5.1 Comparison of fault current for different load percentage	38
---	----

Abbreviations

AC	Alternate Current
CT	Current Transformer
DC	Direct Current
DERs	Distributed Energy Resources
DG	Distribution Generation
FRT	Fault Ride Through
LG	Line to Ground
LLG	Line to Line to Ground
LLLG	Line to Line to Line to Ground
LVRT	Low Voltage Ride Through
MPPT	Maximum Power Point Tracker
OCR	Over Current Relay
MW	Mega Watt
PPC	Power Plant Controller
PT	Potential Transformer
POC	Point of Coupling
PSCAD	Power Systems Computer Aided Design
RMS	Root Mean Square
SCC	Short Circuit Current
SPV	Solar Photo Voltaic
VR-OCR	Voltage Restrained Over Current Relay
VSC	Voltage Source Converter

List of symbols

P	Active Power
Q	Reactive Power
I_{sc}	Short Circuit Current
V_{oc}	Open Circuit Voltage
P_{max}	Maximum Power
R	Resistance
V_{pv}	Terminal Voltage of PV
I_{pv}	Terminal Current of PV
V_{dc}	Dc voltage
P_{ref}	Active Power Reference

Chapter 1

INTRODUCTION

1.1 Introduction

Majority of the electricity in the world is generated through conventional generating systems (such as thermal power plants) which produce a huge amount of greenhouse gases(GHG) [1]. These gases have a significant negative impact on the ecosystem. To save the environment and save human life from calamities, it is advised to use emission-less renewable energy systems over conventional energy systems. As societies embrace the shift towards sustainable energy, the integration of renewable resource technologies such as solar photovoltaic (PV) and wind energy is transforming the power system [2].

The adoption of solar photovoltaic (PV) technology is steadily growing with each passing day and is expected to reach a much higher level in the near future. High penetration of renewable energy systems poses various challenges in power systems in terms of protection and stability [3]. Solar PV is interfaced with the grid through inverters. Inverter switches have their thermal constraints which limit the current to a certain rating beyond which they can get damaged [4]. For a conventional Over current relay which works on the magnitude of current, it is difficult to detect the fault. Thus modification of over-current relays needs to be done.

1.2 Background

With the conventional grid system, the fault current contribution is mainly by synchronous machine, which has very huge rotor inertia, thus supplying an enormous amount of fault current which is easily detectable by over current relay. The network topology of the system changes as a result of renewable energy integration, which has implications for conventional protection.

The fault current in power systems can be detected through various relaying methods. Distribution protection is mainly carried through over-current relays (OCRs) [5]. These relay elements detect the magnitude of the current and update their pickup settings. With renewable plants integrated with a grid system, the contribution of fault current level from the main grid at the point of coupling (POC) is reduced causing blinding of protection and there is a bidirectional current flow as the distribution system is no more radial.

All these issues are undesirable and need to be resolved to protect the system.

In this field research is going on and many methods have been already provided. Most of the research methods focus on the magnitude of phase current on the faulted phase which is not always reliable data for the detection of fault when the system is PV integrated.

During a fault condition, the contribution of fault current from PV is very less compared to a synchronous machine. This is due to the fact that PV is interfaced to the grid through inverter switches. As a result, the inverter current is not easily sensed by conventional OCR, which works on high over current. Thus the PV will continue to supply fault current which is not feasible [6]. Also, the conventional relay coordination that is affected due to the PV plant needs is to be resolved, as the PV plant is connected on the distribution side and will not have a specific position, thus changing the overall topology of the system. The above two problems are addressed in this project.

1.3 Motivation

The penetration of today's power systems is high due to the growing trend of distributed energy systems. In this situation, the subject of protection is quite important. There are several ways that DERs affect traditional security measures. Among them, the few challenges are the change in fault current magnitude due to DER, the Blinding of protection, which results in the blinding of the Grid relay at a point of coupling and bidirectional power flow i.e., there is reverse power flow due to DERs thus causes False tripping. Consequently, this makes it compulsory that the distribution system's security should be made adaptable to new penetrations and topologies [7].

The contribution of fault current by distributed energy resources is at par with the nominal current, particularly by PV plants. This makes it the primary concern to detect this fault current on a magnitude basis. Hence, Protection issues need to be resolved, with different protection strategies for the protection and reliability of the power system [8].

1.4 Literature Survey

Solar energy is being used much more frequently to improve energy security and address environmental issues. The effects of distributed energy supplies on traditional security measures are numerous. Blinding of protection leads to blinding of the power system grid relay at the POC. The cause is a change in the magnitude of the fault current caused by DER. False tripping can take place due to power flow in both directions as the system is no more radial[9]. Consequently, the distribution system's security should be made adaptable to new penetrations.

Many distributed generating systems are interfaced with inverters, including solar PV. The stability

and protection of the power system are significantly impacted by those converters. These inverter switches with thermal constraints limit the fault current for their own protection when a fault arises in the system. Only 1.2–1.5 times the inverter’s rated current can be contributed by inverter-based DGs as fault current [10].

Overcurrent relays (OCRs) are used to protect distribution systems for a very long time. The usage of traditional phase over-current relays is limited by the solar PV system’s limiting fault current contribution feature. Additionally, the fault current contribution from SPV has the potential to partially conceal the main grid’s fault current contribution, delaying the operation of relays mostly at the point of common coupling where DER is connected. These highlighted issues are the limitations of the phase over-current relay that need to be modified.

Various fault detection techniques have been explored in the literature as alternatives to current-based approaches for PV-integrated distribution systems, utilizing phase current and phase voltage. One such method, presented in [11], suggests a voltage-controlled over-current relaying method where the protection algorithm is triggered by the magnitude of phase voltage. However, this method faces limitations when the faulted phase voltage exceeds the threshold due to high fault resistance and the associated voltage control strategy employed in the PV plant. Another approach, described in [12], involves utilising both phase current and phase voltage to establish the required threshold. This method, known as the voltage-restrained over-current relay, aims to address the limitations of the previous method. Nevertheless, dynamic loading conditions implemented in the PV plant may result in incorrect relay operation.

Consequently, techniques based on phase quantities are not suitable for fault detection in distribution systems where a PV plant is present. Additionally, the control strategy employed in the inverter controller causes the PV output current to exhibit a leading power factor during a fault, while conventional systems typically have a lagging power factor [13]. This divergence from the conventional angle-based directional principle further restricts the applicability of existing protection schemes.

In an attempt to overcome these limitations, a positive sequence component-based method is proposed for fault detection [14]. Although this method resolves the issues related to control strategies, it fails to detect faults with higher loading percentages, highlighting the remaining challenges in protecting PV-integrated distribution systems.

1.5 Objectives

The purpose of this project is to prevent the PV system from driving the fault current and maintain coordination among relays of different nodes in the vicinity of the fault. Also, the PV should adhere to the grid codes and follow fault ride-through conditions. To develop such a system, the following objectives need

to follow;

- Comprehensive analysis of SPV plant fault current contribution for fault detection.
- To design SPV which adheres to grid codes and supports fault ride-through conditions.
- To develop an adaptive protection technique that is not influenced by the modes of operation and loading conditions of a PV plant.
- To develop a proper coordination scheme of relays during fault

1.6 Outline of Report

The project outline is structured in the following manner. Chapter 2 deals with the operational modes and modelling of solar PV. Chapter 3 discusses the fault current analysis of grid-integrated solar PV. In Chapter 4, protection schemes are implemented. Chapter 5 provides simulation results with a discussion. Chapter 6 discusses the hardware implementation of the project.

Chapter 2

Solar Photo Voltaic system Modelling

2.1 Introduction

A Grid-connected photovoltaic (PV) system primarily comprises a collection of PV modules linked to a converter, which converts DC electrical energy into AC. The level of irradiance and temperature have a significant impact on the output power produced by the PV system. The steps for building up a simple solar farm in PSCAD are described here. The solar farm consists of:

- Power Plant Controller (PPC) is a simplified monitoring system that manages solar PV operations at the Point of Coupling. The PPC modifies the active and reactive power references for the solar farm's inverters using measured parameters like active (P), voltage(V), and reactive power(Q), as well as operating mode (for example, fixed reactive power, voltage, and power factor). It also identifies low-voltage and high-voltage ride-through scenarios. As a result, the overall stability of solar PV and its linked network is improved.
- The PV module is responsible for generating power based on irradiation and temperature levels. It displays why the SPV array's variables may be changed to provide a certain output power under standard temperature and irradiation circumstances. Here in this current project, the PV module generates a maximum power output of 0.25 Mega Watts when subjected to a nominal 1000 W per square metre of radiation and a nominal 28 °C ambient temperature.
- The Boost Converter is used to either achieve the tracking of the highest power point (MPPT) or to regulate the DC voltage.

The inverter is primarily controlled to achieve desired dynamics and control scenarios within the solar farm.

- The Scaling Component is employed to represent multiple inverter units within a solar PV. In this project work, the solar PV comprises 100 number of units. Figure 2.1 above illustrates the overall configuration of integrating solar PV into an operational electrical system [15].

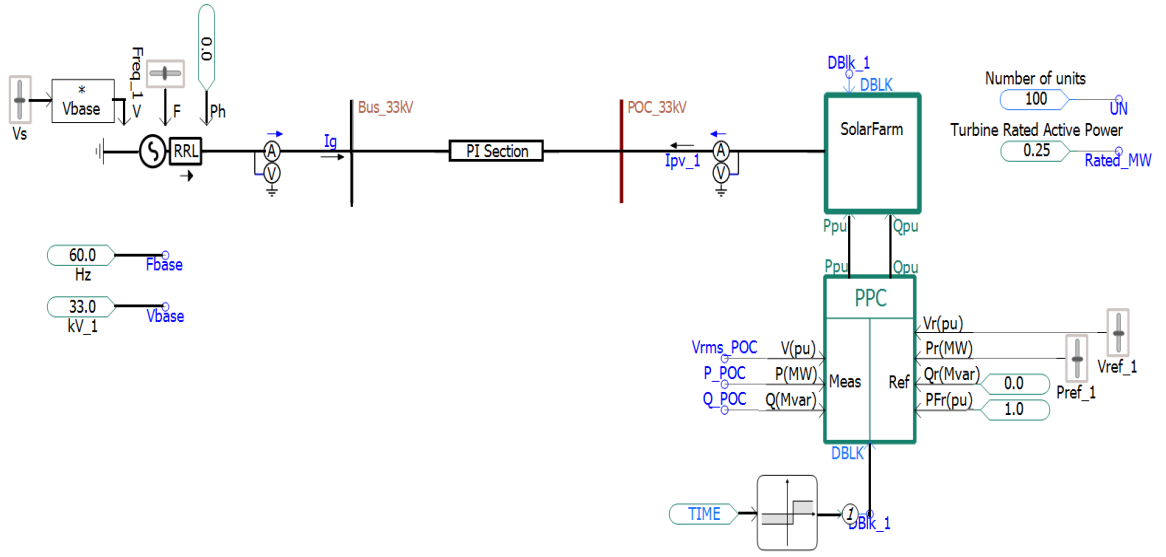


Figure 2.1: Solar farm integrated with power system grid

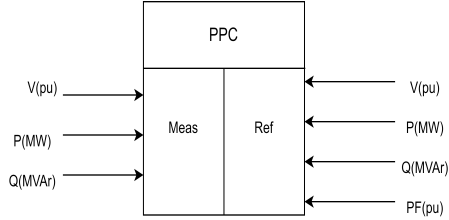


Figure 2.2: Power plant controller

2.2 Power Plant Controller

Figure 2.2 depicts the Power Plant Controller, which is responsible for generating P and Q references for solar PV. These references are determined based on the measured quantities and reference values. Figure 2.3 displays the input parameters of the Power Plant Controller (PPC). The "con-mode" option is used to choose one of the operating modes: power factor(PF) control, voltage control and or fixed reactive power (Q) control.

2.3 SPV module Setup

The PV array serves the purpose of obtaining significant characteristic quantities, including the open circuit voltage (V_{OC}), short circuit current (I_{SC}), and max. power (P_{MAX}) of the PV module. These particulars are necessary to set up the Boost controller. Figure 2.4 illustrates the circuit configuration used to measure these quantities.

In order to measure the mentioned quantities, the resistance (R) is systematically adjusted from a nearly negligible value of 0.001 ohms to an extremely high value, as shown in Figure 2.5, representing the open circuit condition, as the simulation progresses over time (TIME). This varying resistance (R) causes corresponding

Name	Caption	Type	Unit	Value
Scale	Number of Inverters	Integer	UN	
Sbase	MVA Rating of Single Inverter	Real	MVA	Rated_MW
con_mode	Reactive Power Control Mode	Choice		1
HVRT	HVRT Detection Threshold	Real	pu	1.15
LVRT	LVRT Detection Threshold	Real	pu	0.85
Pmax	Pmax	Real	pu	1
Pmin	Pmin	Real	pu	0
Qmax	Qmax	Real	pu	0.6
Qmin	Qmin	Real	pu	-0.6

Figure 2.3: Input parameters of PPC

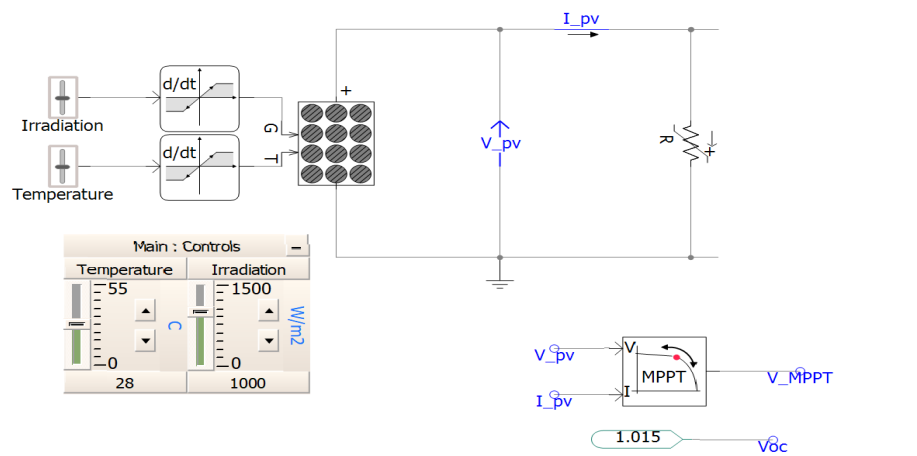


Figure 2.4: Circuit configuration for measuring Open circuit voltage , short circuit current and maximum power of SPV module

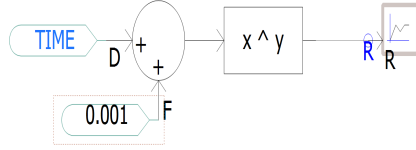


Figure 2.5: Variation of resistance with simulation time

changes in the terminal voltage (V_{pv}) and current (I_{pv}) of the PV array. Figure 2.6 exhibits the changes in resistance (R) throughout the simulation duration and illustrates the corresponding fluctuations in V_{pv} and I_{pv} . Notably, the P_{MAX} observed is approximately 0.25 MW, the V_{OC} measures around 1.015 kV, and the I_{SC} amounts to approximately 0.325 kA. By adjusting the characteristic parameters of the PV array, it is possible to modify quantities such as the P_{MAX} , V_{OC} , and I_{SC} . To make these modifications, double-click on the PV array component, which will allow edit parameters such as the number of cell modules and photo voltaic cells within the PV arrays. References for temperature (28°C) and irradiation (1000 W/m²) can be done through the interface shown in Figure 2.7.

2.4 Controller units and circuit layout of solar farm

Figure 2.8 illustrates solar PV, showcasing the implementation of power electronic circuits and controllers. The specific parameters can be seen in Figure 2.9.

2.4.1 SPV Boost Converter

The boost converter, depicted in Figure 2.10, incorporates the PV array as its input. Figure 2.11 represents the controller used in the system. The controller offers two selectable control modes, which can be alternated using a switch. The two control modes are described as follows:

- DC voltage control mode is the initial control mode. The controller controls the DC voltage in this mode so that the voltage source converter (VSC) is able to effectively regulate the active power on the DC connection. When prioritising reactive power control for the VSC, this mode is frequently used.

Second control mode is the MPPT control mode. In this mode, the controller utilizes the important characteristic quantities of the PV array, such as I_{SC} , V_{OC} , and P_{MAX} , to optimize the power output and follow the PV system's maximum power output. This control mode is primarily employed when prioritizing active power control for the VSC.

2.4.2 Voltage Source Converter

The Voltage Source Converter (VSC) is specifically designed to control either the DC voltage (V_{dc}), P and or Q. The switch is provided to choose between the two. There are various controllers which are used to control and generate converter references. The overall PV module is shown in Figure 2.12.

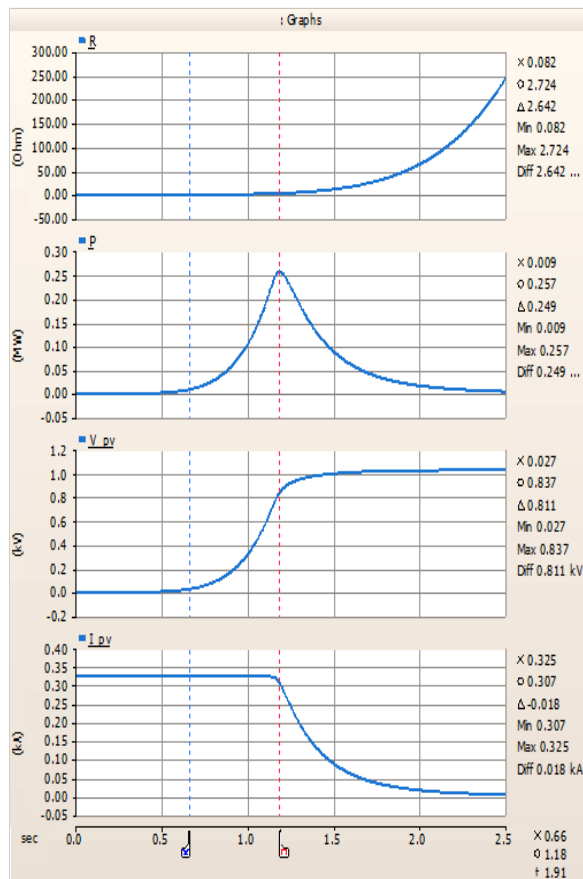


Figure 2.6: Variation of SPV parameters as a function of resistance variation

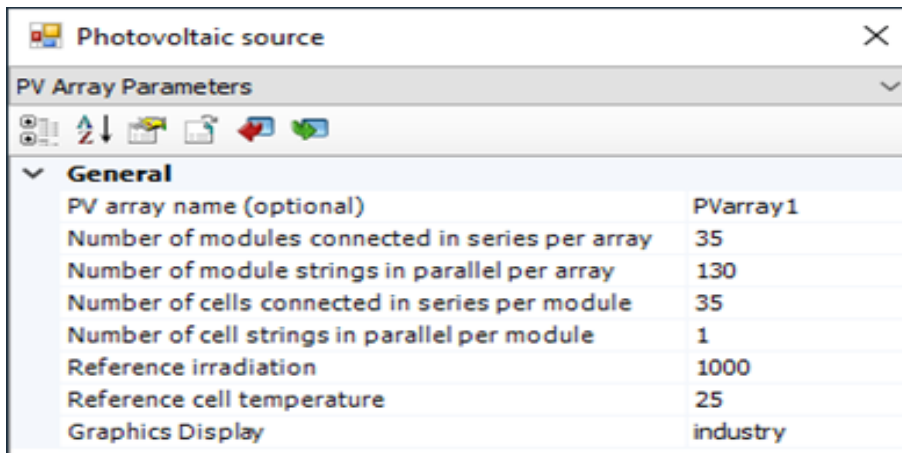


Figure 2.7: Configuration of SPV array

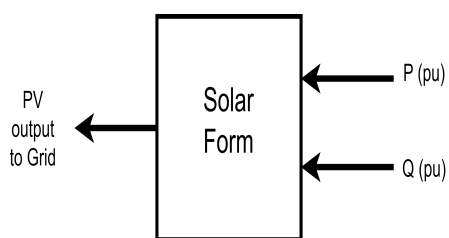


Figure 2.8: Overall Solar farm module

Base Values and Limits	
Number of Inverters	UN
Inverter S base (MVA)	Rated_MW
Medium Voltage Base (kV, rms, 3ph)	Vbase
System frequency (Hz)	Fbase
Limits	
Priority	P
P max	1.0 [pu]
P min	0 [pu]
Q max	0.6 [pu]
Ramp Rates	
Real power ramp rate (pu/s)	1.0 [pu/s]
Reactive power ramp rate (pu/s)	1.0 [pu/s]

Auxiliary Control Schemes	
Enable P(f) Mode	Enable
Deadband	0.4 [Hz]
Slope of P Curve Outside of Deadband (pu/Hz)	0.45 [pu/Hz]
P(f) Ramp Rate	0.5 [pu/s]
VRT Mode	
Enable VRT Q Offset	Enable
Deadband	0.2 [pu]
Slope of Iq Curve Outside of Deadband (pu/pu)	2.5

Figure 2.9: Solar Farm input parameters

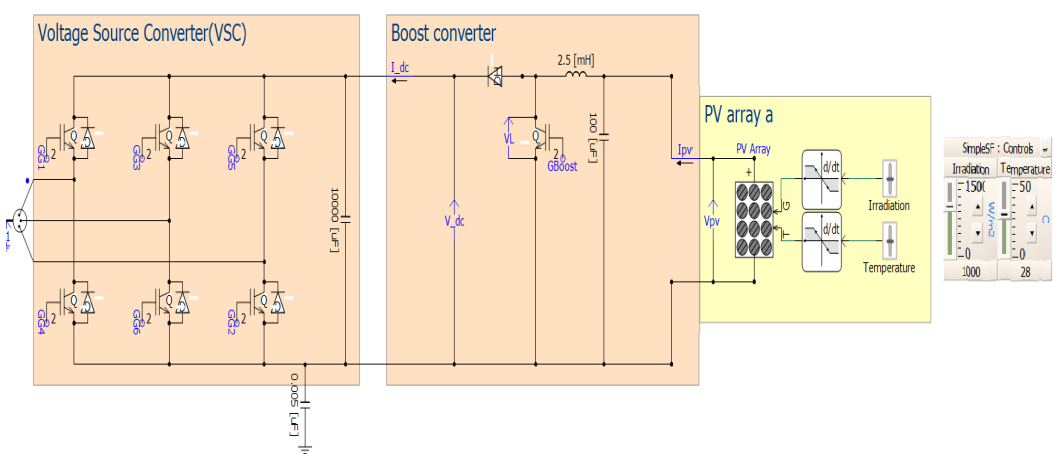


Figure 2.10: Boost converter connected to SPV array

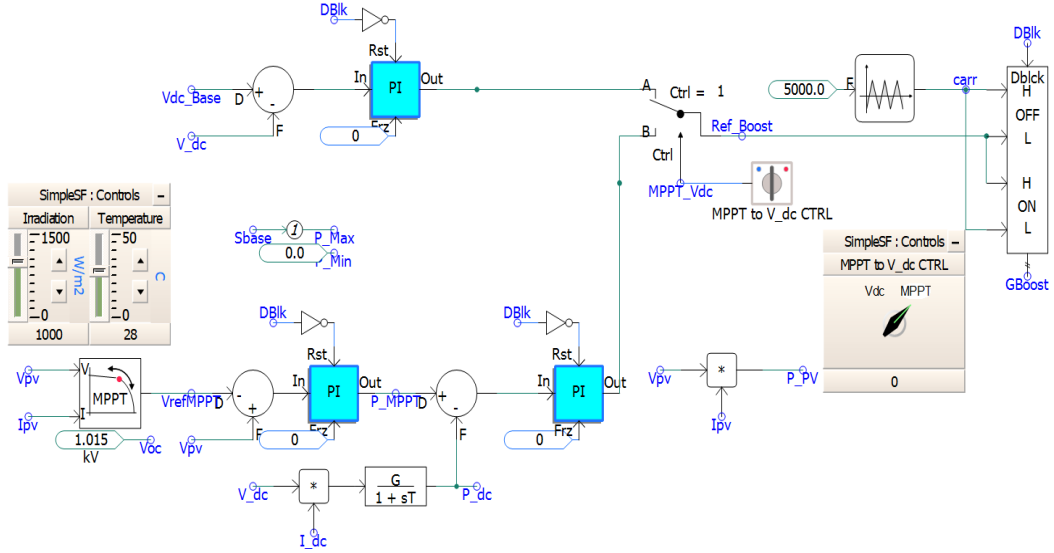


Figure 2.11: Boost controllers

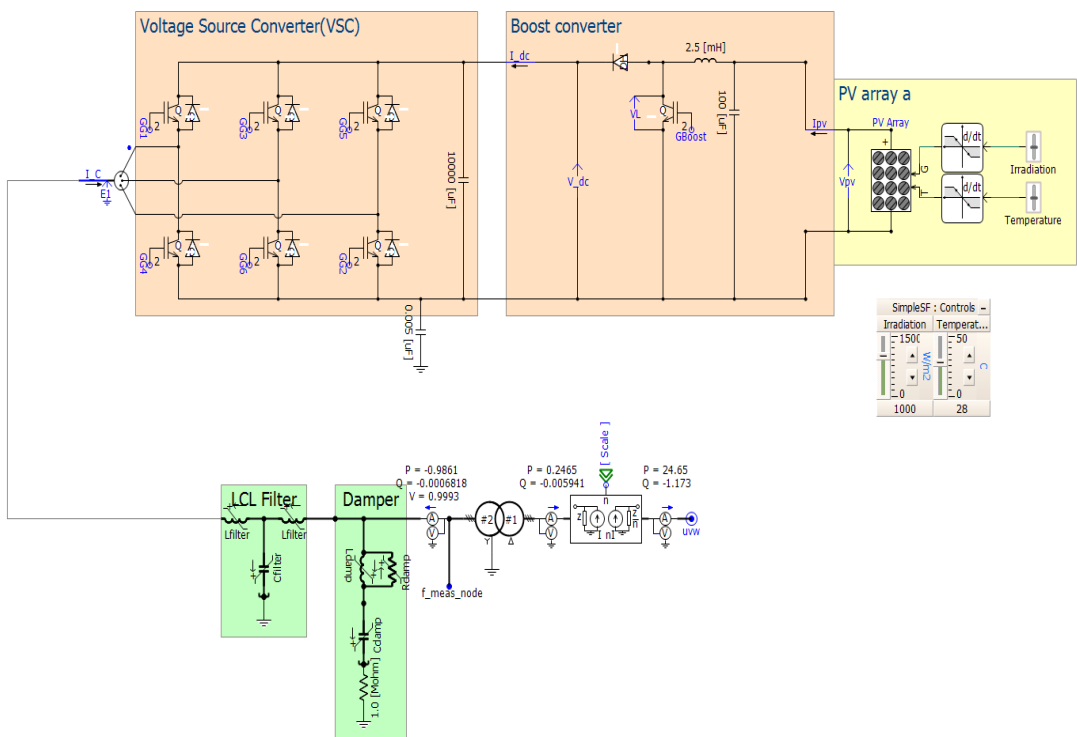


Figure 2.12: PV module consisting of PV array, Booster converter, VSC, LCL Filter, and Damper respectively

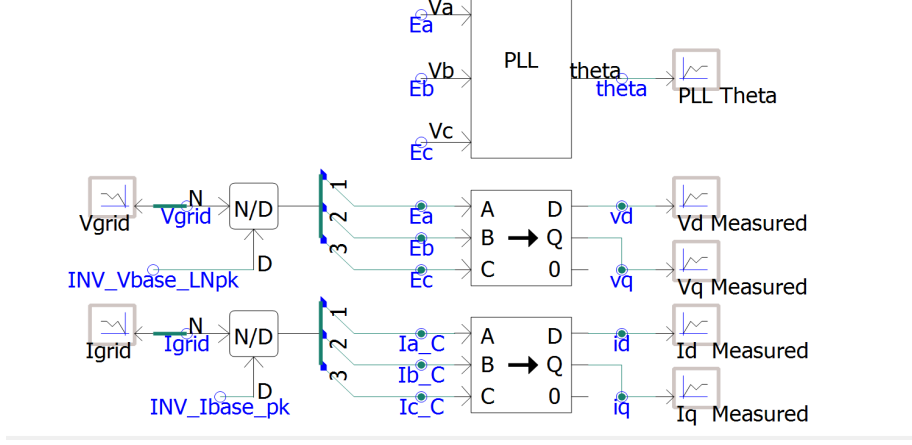


Figure 2.13: Phase Lock Loop and the ABC-to-dq transformation

2.4.3 PLL and ABC-to-DQ0 Transformation

Since solar PV operates in a grid-tied scheme, a Phase-Locked Loop (PLL) is necessary to determine the accurate phase angle of the bus voltage at the Point of Connection. This phase angle information is crucial for various control and synchronization purposes. Figure 2.13 illustrates the utilization of the measured phase angle (θ) to derive the voltage and current's d-q components using the ABC-to-dq transformation. This transformation facilitates the representation and control of the electrical quantities in a rotating reference frame, simplifying the control strategies employed in the solar farm. The inverter is designed to offer control over the V_{dc} or P and Q. A switch within the system, as depicted in Figure 2.14, enables the selection between controlling the DC voltage or active power. In the case of active power control, a reference value for P is determined by a frequency droop characteristic, shown in Figure 2.15. As the frequency measured (PLL_f) surpasses the nominal frequency (systemFreq), the reference P is adjusted within a certain range, which is influenced by the slope of the deadband controller. This mechanism ensures the active power output varies proportionally with changes in frequency, maintaining stability within the system [16].

The inverter current is restricted through the limitations of the PI controllers. The selection of the limit function is determined by the priority signal and can be set to prioritize either P or Q, as illustrated in Figure 2.16. This allows for controlling the inverter current based on the desired power priority.

Furthermore, to ensure the inverter's ability to operate during low-voltage ride-through events, The inverter's maximum current rating is 1.5 pu (per unit). This rating enables the inverter to handle and sustain operation under conditions of low voltage without compromising its performance and stability. The reference voltages for the converter, v_d and v_q , are produced by the inner current controls shown in Figure 2.17. To achieve the decoupling of the d- and q-frames and minimize their mutual influence, the terms $I_d * L_{pu}$ and $I_q * L_{pu}$ are subtracted from and added to the q-frame and d-frame, respectively. This decoupling technique helps to minimize the cross-coupling effects between the d- and q-axes, allowing for more independent control of the current components. Figure 2.18 showcases the time domain voltage references (Ref_a , Ref_b , and Ref_c) derived from the phase domain voltage references. The action starts with the conversion of rectangular

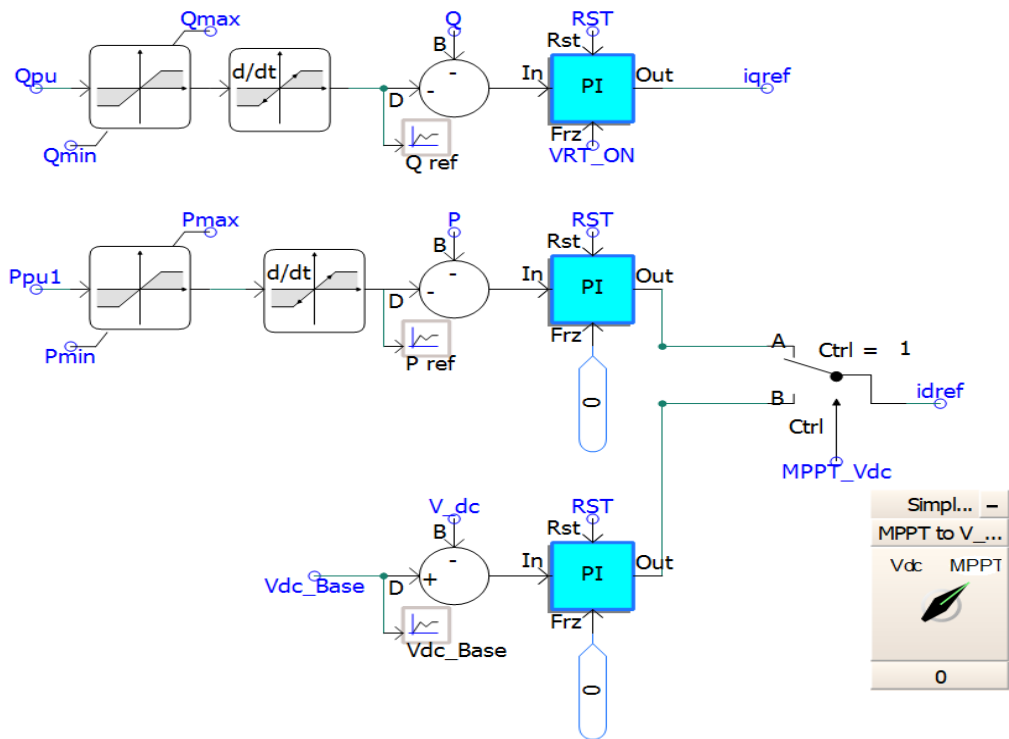


Figure 2.14: Outer controllers

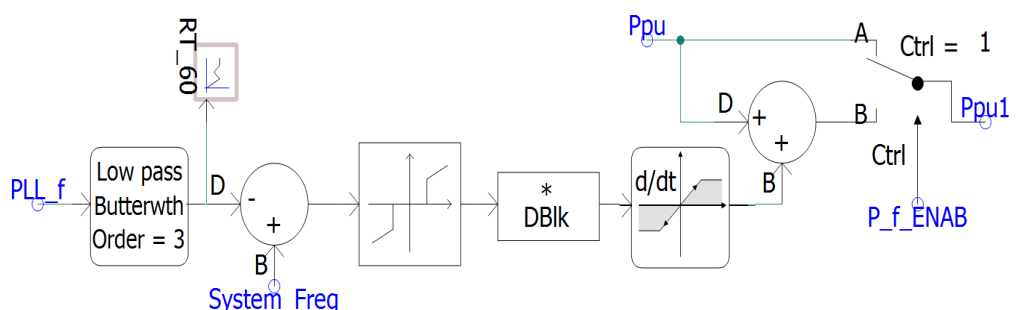


Figure 2.15: Frequency droop characteristic and the dead band controller

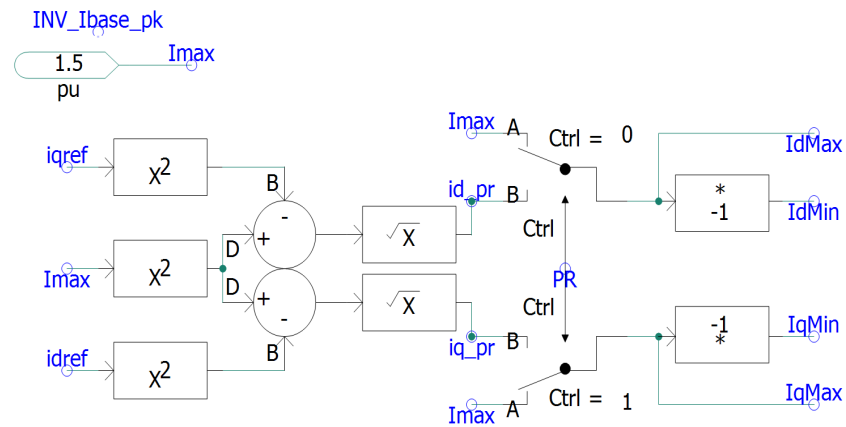


Figure 2.16: d- and q-frames current limit calculation

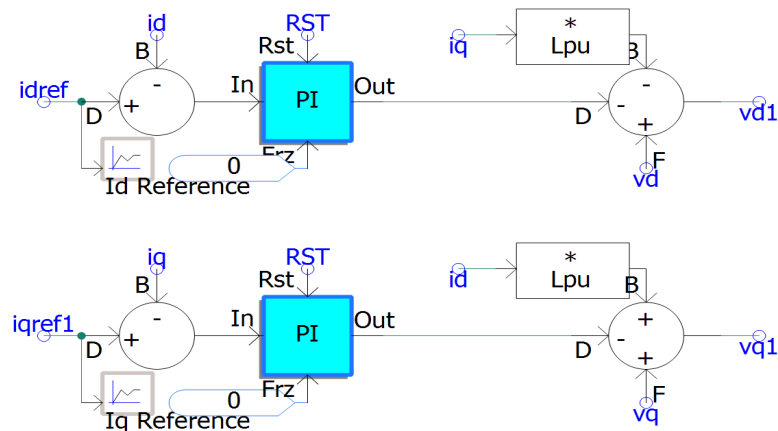


Figure 2.17: Inner current controllers and decoupled components

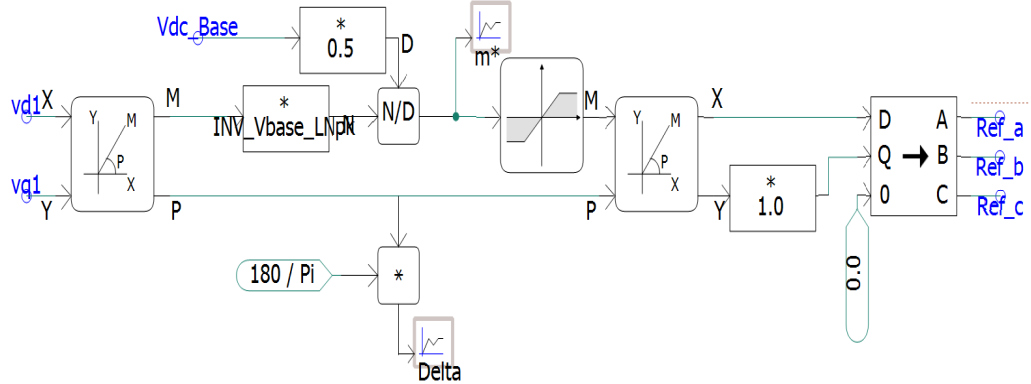


Figure 2.18: Reference voltages provided by grid-side controller

coordinates to polar coordinates. The modulation index (m^*) is then restricted to a maximum of 1.15 pu after the magnitude (M) is divided by 0.5 Vdc Base. In order to apply the polar coordinates to the dq-to-ABC transform component, the polar coordinates must first be transformed back to rectangular form. By utilizing theta angle generated by the PLL, it is possible to acquire the voltage three-phase reference waveforms. This process ensures the generation of appropriate voltage references based on the desired characteristics and control requirements of the system.

2.5 Fault Ride-Through (FRT)

In the distribution system, most faults are temporary in nature, often caused by events like lightning strikes. In order to correct such problems, the power system is built to automatically stop the line circuit to restore the circuit when the fault has been corrected. The goal of this strategy is to achieve a delicate balance between being able to "ride through" momentary problems and disconnecting from persistent issues.

System operators are faced with the difficulty of keeping control over the overall power generation linked to the system as Distributed Energy Resources (DERs) penetration levels rise. In particular, at high penetration levels, it might cause serious voltage and dynamic stability issues if DERs are forced to disconnect for all fault circumstances. Before going offline, conventional synchronous generators may ride through brief voltage drops in the gearbox system. Grid operators now require all generators, including wind turbines, to have "low-voltage ride through" (LVRT) capabilities [17] to allay this worry. In order to offer post-fault voltage support and promote grid stability, LVRT standards make sure that generating facilities stay connected during temporary fault scenarios. The stability, dependability, and security of the electric power network are all priorities for these needs.

2.6 Summary

In this chapter, the implementation of solar PV is explained, and along with that, different components of PV module such as voltage source converters (VSC), boost converters, and PV array are briefly

explained. Also, the overall control design of solar farm is explained along with a block diagram. In the coming chapters, the operation of solar PV in a grid-integrated system along with fault analysis will be discussed.

Chapter 3

Fault Analysis of Grid Integrated Photo Voltaic

3.1 Introduction

The modelled solar PV created in PSCAD is working in the following modes of operation

- Power Plant Controller can operate in various modes of operation, such as fixed reactive power mode, power factor mode, and voltage control mode. In this work, PPC is set to operate in voltage control mode,
- Boost converter can operate DC voltage mode and MPPT mode. In this work it is set to operate at MPPT mode.

3.2 PV-Integrated Grid

The PV-integrated grid model, as shown in Fig.2.1, is a simulation model created in PSCAD for analysing the fault currents. This model incorporates a solar photovoltaic (PV) system and a grid, operating at a reference voltage of 33 kV and a frequency of 60 Hz. The solar PV system has a capacity of 25 MW, while the grid has a capacity of 100 MVA. From Figure 3.1, it is observed that PSV supplies an active power of 25 MW and reactive power of zero under nominal conditions. The root mean square (RMS) voltage level is 1 pu and the RMS current of 0.435 pu can be seen in Figure 3.2.

In order to represent the distribution system, a PI-section model of the transmission line is utilised. This model is suitable for medium voltage levels and helps simulate the behaviour of the power flow in the system.

During the simulation, normal load conditions are simulated, and the multimeter device is used to measure various system parameters. These parameters include voltage, current, active power, and reactive power. The multimeter allows for accurate monitoring and analysis of the system's electrical characteristics during the simulation. It is important to note that the SPV system functions in MPPT mode, which means it always supplies the rated available power. By gradually increasing and decreasing the load on the system, the behaviour of the PV system becomes evident. Despite the changes in load, the solar PV system consistently

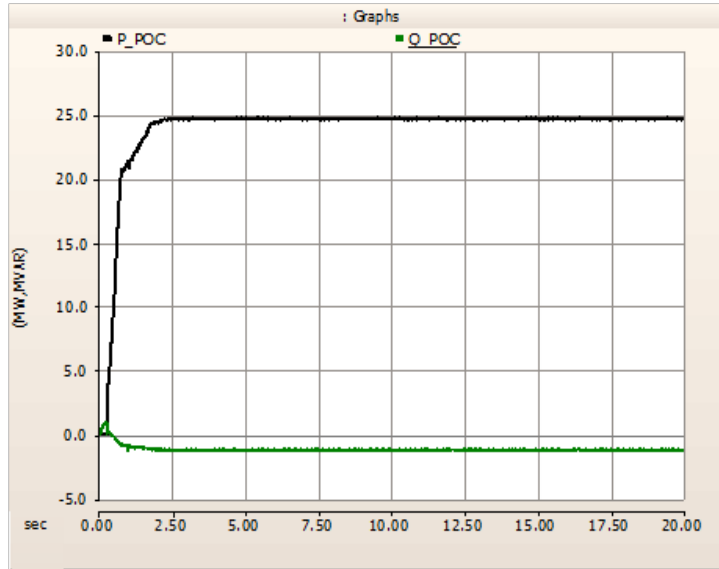


Figure 3.1: Active power and Reactive power supply by PV in nominal condition

delivers the rated power. This observation demonstrates the effectiveness of the MPPT mode in optimising the PV system's performance. In this work, P_{ref} is set at 25 MW. Thus irrespective of loading conditions, the PV is delivering 25 MW.

3.3 Fault Characteristics of Inverter-based DER

Synchronous and induction machines differ from inverters in their dynamic behaviour. Unlike synchronous and induction machines, inverters lack a rotating mass component, which means they don't possess the inertia to carry fault currents based on electromagnetic characteristics. In inverter-based resources, fault currents exhibit a rapid decay in their envelope, due to the absence of predominantly inductive characteristics found in rotating machines. The characteristics of fault currents are influenced by the time constants inherent in the circuit. Inverters offer a level of control that is distinct from rotating machines. These control parameters affect the fault current characteristics of the inverter, further differentiating it from synchronous and induction machines.

The interface between the Distributed Energy Resource (DER) and the utility system connection can utilize either a voltage control scheme or a current control scheme. In both schemes, a DC link capacitor is used to ensure voltage stability during transient conditions. In the voltage control scheme, the DER exhibits a higher initial current overshoot, meaning that the current rises quickly during the transient period. On the other hand, in the current control scheme, the increase and decrease of current back to steady-state values occur at a slower rate. When the DER operates under a voltage control scheme, it tends to contribute more to faults during the transient period, which typically lasts around the first 5-10 cycles (Baran and El-Markaby, 2005).

Inverter-based Distributed Energy Resources (DER) possess a unique characteristic related to their

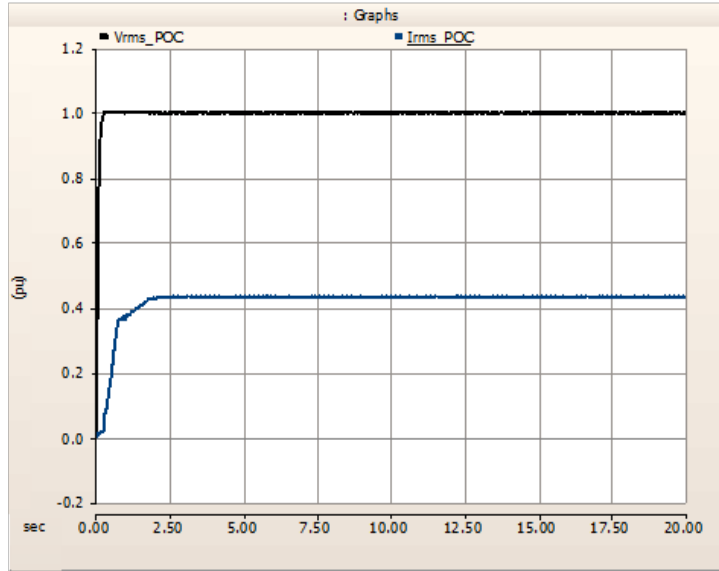


Figure 3.2: Per unit voltage and current supplied by PV during nominal condition

power electronics interface, which enables the control of fault current contributions from these systems. This adjustability offers an opportunity to optimize the coordination of system protection by regulating the levels of fault currents (Iravani, and Tang 2005). The design of inverter-based DER is done to function as ideal current sources, resulting in minimal contributions to fault currents and minimal impact on the protection and coordination strategies of fuses and circuit breakers (GE, 2003). However, as the penetration of DER increases, reaching 10 percent or more, this may no longer hold true (GE, 2003; El-Markaby and Baran, 2005).

3.4 Inverter Operation Under Fault Conditions

3.4.1 Symmetrical Fault (LLLG)

The fault current is often quite large during symmetrical faults, which happen when all three phases of a power system are linked to the ground. Usually, external factors like broken trees that create a short circuit path to the ground are to blame for these failures. The resistance of the ground fault itself is the main factor limiting the fault current. The short circuit is limited by the transformer and line impedances, assuming the short circuit is complete.

Effective system protection mechanisms are put in place to safeguard transformers and other parts connected in series with the fault, with circuit breakers playing a key role in promptly clearing the fault to avoid damage from high short-circuit currents. The negative and zero sequence components are often ignored when analysing three-phase faults since only the positive-sequence circuit is symmetrical [18].

Due to the symmetrical nature of faults in three-phase systems, it is crucial to realise that neither the grid nor the photovoltaic (PV) inverter contributions to the fault have negative or zero sequence components.

However, transient currents may momentarily include negative and zero sequence components in both the grid and PV inverter contributions during the beginning and terminal stages of the event. The major focus is on the grid's considerable rise in SCC when it enters fault condition, notwithstanding these transitory changes. The PV inverter's current controller limits the SCC from the inverter (I_{INV1}) to I_{max} .

Unsymmetrical faults, which are more common than symmetrical faults, can involve various fault types. These faults can include ground faults like SLG (single line-to-ground) faults and LLG (line-to-line-to-ground) faults, or they can occur between two lines (LL) without involving the ground. The presence of an SSC path to the ground significantly impacts the contribution of the short-circuit current during unsymmetrical faults. Furthermore, the winding connections of transformers and generators have an impact on the flow of zero-sequence current [19]. Zero-sequence current cannot flow via some winding arrangements, such as delta or floating wye (Y) connections. In some installations, a small reactor (Z_n) is incorporated to ground the neutral point of Y-connected windings, intentionally impeding the zero-sequence current. These measures help manage the effects of unsymmetrical faults and maintain system stability.

Under unsymmetrical fault conditions, both solar photovoltaic (SPV) systems and the grid contribute to the fault current, containing all sequence components of currents. However, the grid tends to have a higher content of negative sequence components compared to SPV systems [20]. On the other hand, the zero sequence component is negligible in SPV systems compared to the grid.

It is worth noting that SPV systems always supply balanced current to the grid, regardless of fault conditions. As a result, the positive sequence component becomes the main data for fault detection from the SPV distribution side.

3.5 Summary

In this chapter we have highlighted the modes of operation of the solar farm. In the later part of this chapter, we talked about the fault current characteristics of the solar farm and their fault current contribution to different types of faults. Where we got to know that they supply balanced current irrespective of the conditions whether normal or fault current.

Chapter 4

Overcurrent Protection of distribution systems

4.1 Over-Current Protection

The over-current relay (OCR) is a fundamental protective device that continues to be extensively used in various applications across power system operations. Its primary function is to activate when the current flowing through a circuit exceeds a predetermined threshold. This threshold is set based on the permissible current levels to ensure the safe operation of the system and protect it from damaging overloads or short circuits [21].

Overcurrent relays can be categorised into two types: instantaneous relays and time-overcurrent relays. Instantaneous relays have no intentional time delay and provide immediate tripping of the circuit breaker when the current exceeds the set value. On the other hand, time-overcurrent relays exhibit a characteristic operating curve that varies with time. Figure 4.1 depicts the general operational behaviour of a time-overcurrent relay.

The characteristic curve of the relay is inversely proportional, implying that as the current magnitude rises, the relay's operating time decreases. This behaviour allows the relay to respond rapidly to higher fault currents, minimising potential damage to the system.

Compared to other types of protective relays, overcurrent relays are relatively simple in their operation. They rely on the measurement of just one system variable, which is current, to initiate their protective function. By continuously monitoring the current magnitude, overcurrent relays can detect abnormal or excessive currents and take appropriate action to isolate the faulty section of the system.

Despite their apparent simplicity, overcurrent relays offer a wide range of possibilities in terms of relay characteristics. By manipulating the variables of current and time, different operating characteristics can be developed. These characteristics define the response behaviour of the relay and determine factors such as the tripping time for various current levels.

The selection of the appropriate relay characteristic depends on the specific application requirements and the need for coordination with other protective devices within the power system. For example, coordination

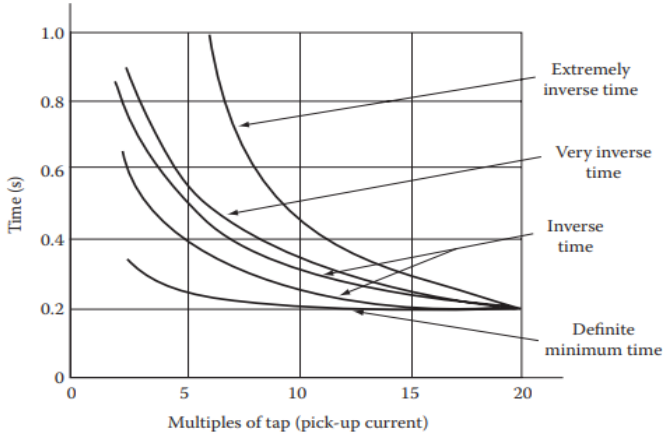


Figure 4.1: Characteristics of inverse-time-over-current relay .

with fuses or other relays ensures that the protective devices operate in a coordinated manner to isolate faults accurately while minimizing disruptions to the rest of the system [18].

4.2 Extremely Inverse Over-current Relay

Inverse-time overcurrent relays exhibit a unique operating characteristic in which their response time decreases as the current magnitude increases. This characteristic is particularly advantageous in situations where high fault currents need to be swiftly detected and isolated to prevent damage to the power system.

To cater to the diverse requirements of different applications, inverse-time OCRs are available in various characteristics, such as inverse-, very inverse-, and extremely inverse-time characteristics. These characteristics define the specific relationship between the time of operation and the current magnitude.

The inverse-time characteristic implies that as the current exceeds the relay's set threshold, the operating time of the relay demonstrates an inverse proportionality to the magnitude of the current. In other words, higher currents result in shorter operating times. This characteristic is suitable for applications where fast fault detection and isolation are crucial to prevent extensive damage.

Very inverse-time characteristics exhibit a more pronounced inverse relationship between the operating time and current magnitude. They provide even faster response times for higher currents, ensuring rapid fault clearance and enhanced system protection.

Extremely inverse-time overcurrent relays are primarily utilized in distribution systems that incorporate renewable energy plants. This choice is attributed to the limited fault current contribution from renewable energy sources. Renewable plants typically have lower fault current levels compared to conventional power sources. By employing extremely inverse characteristics, these relays can accurately detect faults even at lower fault current levels, ensuring reliable protection for the distribution system.

By selecting the appropriate inverse-time characteristic, power system operators can tailor the relay's response to match the specific needs of their application. Whether it's protecting transmission lines, dis-

tribution systems, or renewable energy installations, the inverse-time overcurrent relays offer flexibility and efficiency in fault detection and clearance, contributing to the overall reliability and stability of the power system [22].

4.2.1 Fault Detection

A line-to-ground (LG) fault is introduced between bus-2 and bus-3 of the IEEE 9-bus system as shown in Figure 4.2. The IEEE 9-bus system is a test bed for designing relay characteristics. The fault current of

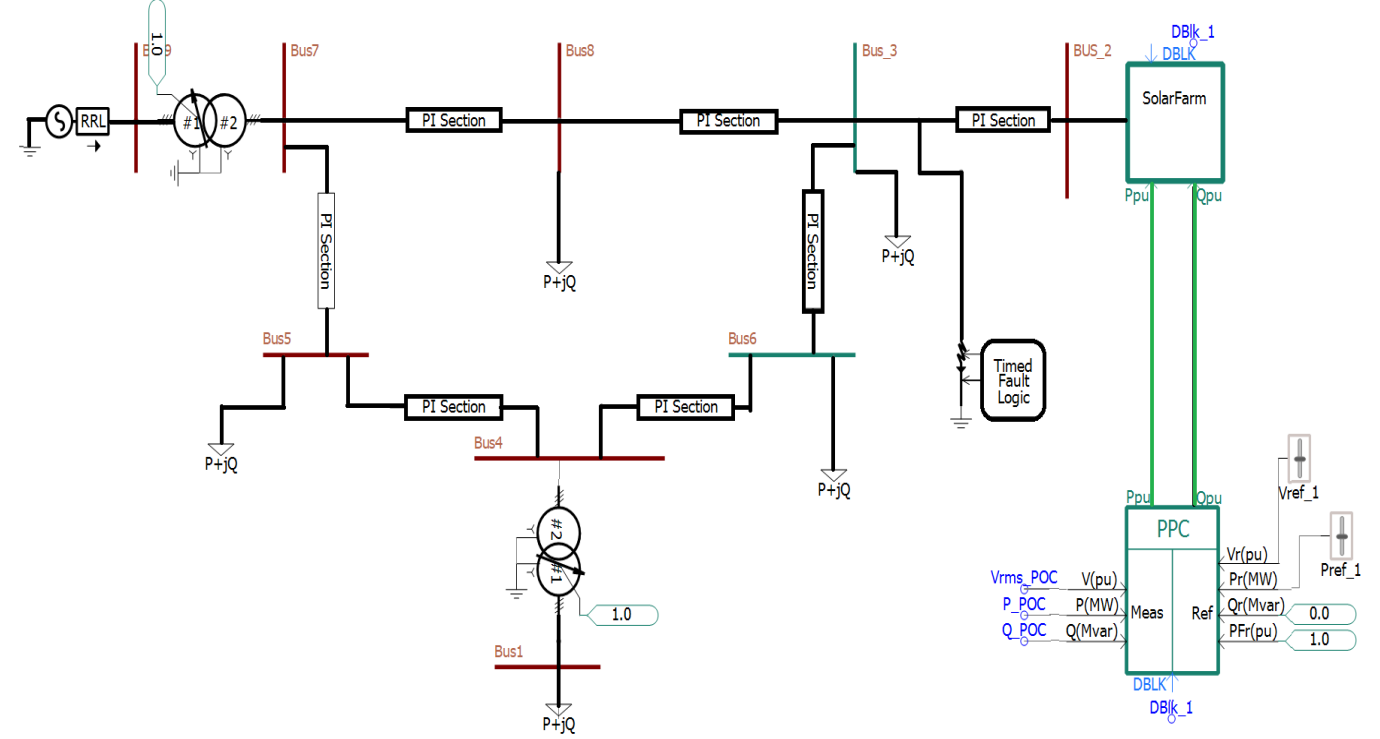


Figure 4.2: Simple 9-Bus system with LG fault at bus-2

solar PV is taken from a multimeter reading and the fault current is found to be 1.55 times the full load current. An Extremely Inverse Definite Minimum Time over current is used to sense the magnitude of fault level. The fault current to the over-current relay is fed through a current transformer with a specified current ratio of 1000/1.

The positive sequence component of fault current from PV is used for fault detection. The sequence components are obtained through Fast Fourier Transformation(FFT) block which takes input as three phase supply and calculates the FFT preliminary output through a block called a sequencer, the output of the sequencer block includes the magnitude and phase components of the fundamental positive (+), negative (-), and zero-sequence, as well as the corresponding components of each harmonic. Additionally, the system provides the DC components of each phase.

As the fault is detected in the relay a delay time is added in the relay circuit to bypass the transients or DC offset current. The output of the relay is provided to the circuit breaker through a signal element.

The circuit breaker trips the circuit and isolates the PV from the faulted section. The relay logic developed is shown in Figure 4.3. It has been found that the time of operation of the PV side relay takes more time to trip than the grid side relay. This is because of the limited current contribution from PV. The trip time or time of operation is calculated by

$$t_{trip} = T_D \left(\frac{A}{M^p - 1} + B \right) + K \quad (4.1)$$

where A, B, and K are constants and have default values of the PSCAD relay. T_D is the time dial setting and M^p is the Time multiplier setting. . The results are discussed in the next chapter. In order to decrease the operating time of the PV side relay, we are going to take pickup current as a function of voltage.

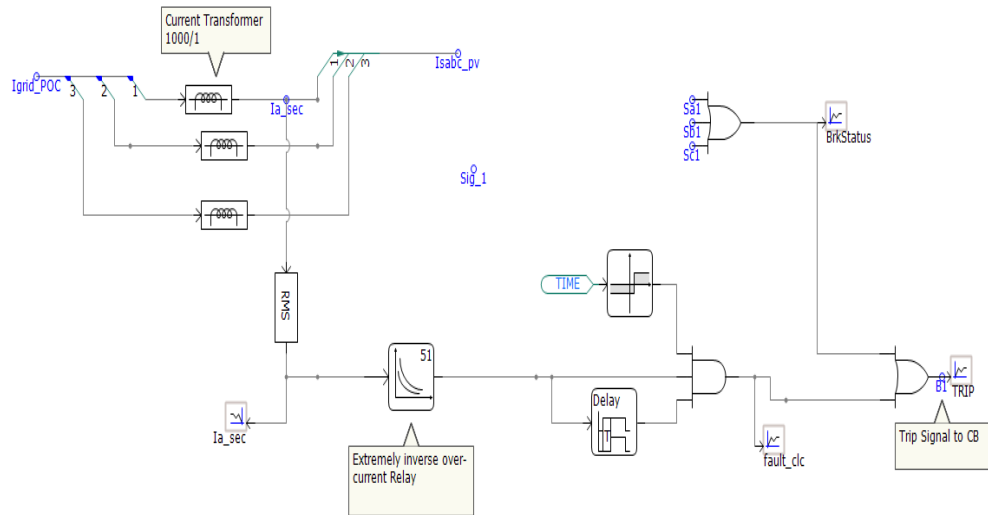


Figure 4.3: Shows the relay logic of OCR and breaker status circuit

4.3 Voltage-restrained Over-current Relay

By creating a proportional relationship between the set overcurrent operating value and the input voltage, voltage-restrained overcurrent protection improves the sensitivity of overcurrent relaying. In many cases, these relays are used in place of impedance relays with small- to medium-sized generators (5–150 MVA). Voltage-restrained overcurrent relays are also used in networks where, in comparison to conventional overcurrent relays, they offer better coordination and fault detection. This is especially useful in situations where diverse fault current sources might cause fault currents to fluctuate and fall below the typically rated line current. These relays' working times may be customised using one of five distinct inverse curves or a set time delay. When the inverse time delay option is used, the applied current and the input voltage applied within the defined voltage range determine the delay duration. As a result, a reduction in voltage, in addition to an increase in current, shortens the operating delay. In Figure 4.4, it can be seen that the pickup value of VR-OCR decreases with a decrease in voltage at the fault bus, thus reducing the tripping time of the Relay. The Relay logic of VR-OCR is shown in Figure 4.5. The results obtained are validated and discussed in the

next chapter.

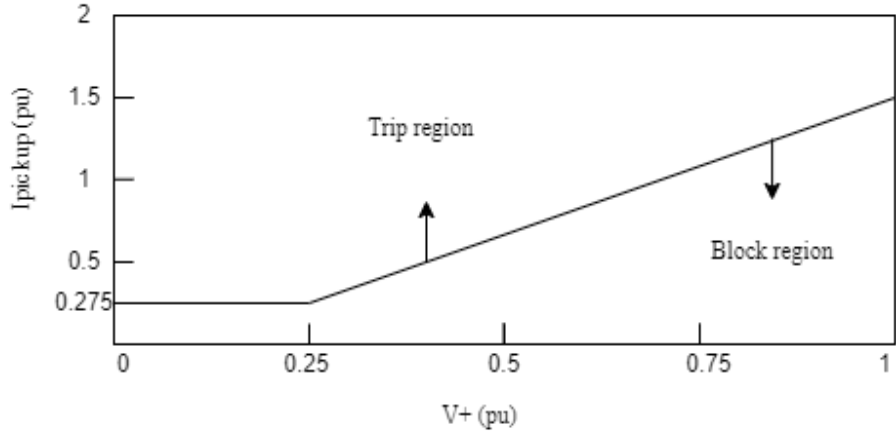


Figure 4.4: Conventional tripping characteristics of VR-OCR

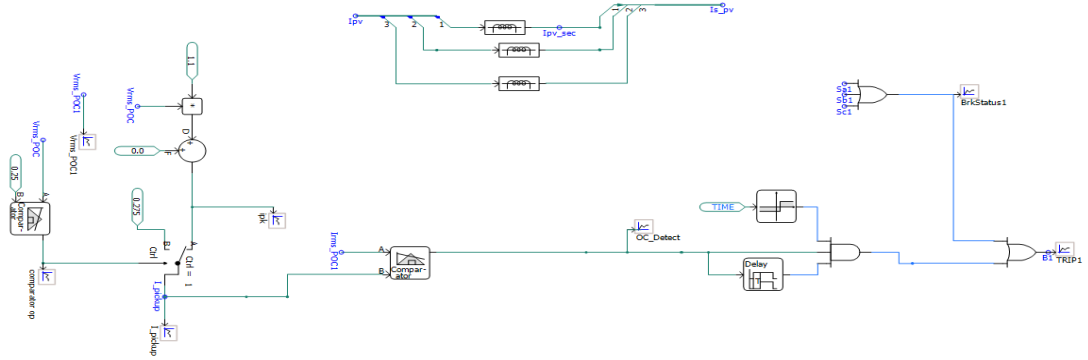


Figure 4.5: Shows the relay logic of VR-OCR and breaker status circuit

4.3.1 Effect of loading percentage on relay current

Voltage-restrained overcurrent relays work adaptively for different types of faults. The adaptive nature is observed in the sense that it updates its current pickup values as per the change in bus voltage. The fault current level of PV has been observed to change with different loading percentages. In Figure 4.6, the PV bus is loaded first with 100 % loading, a fault is created at bus-2 of the PV integrated grid system, and fault current is measured at bus-3 of the system. Again, the same process is repeated with a loading percentage of 50% and without a load condition.

Observations indicate that as the percentage loading increases, the pre-fault current detected by the relay decreases. Consequently, there is a need to modify the voltage-restrained overcurrent relay so that it can adaptively operate under varying loading conditions. Hence, an adaptive voltage-restrained overcurrent relay (OCR) characteristic is suggested as a means to safeguard the distribution line that links the inverter-interfaced PV plant. This method utilizes the input voltage magnitude to dynamically modify the tripping characteristics, taking into account the pre-fault current detected by the relay. The adaptive pickup current,

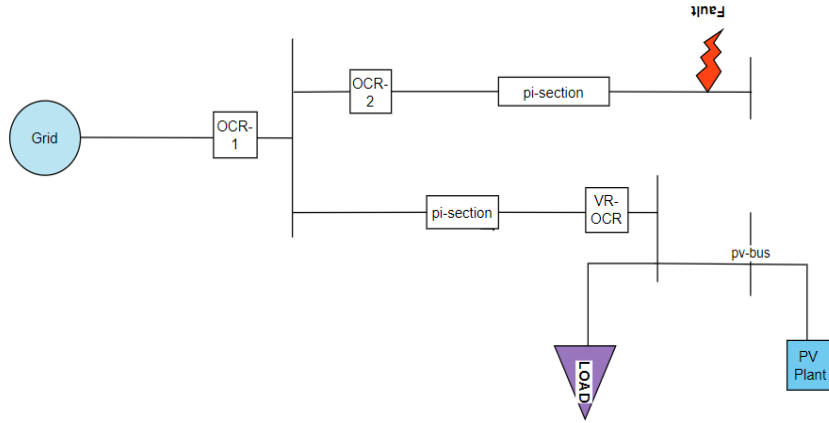


Figure 4.6: A PV plant integrated 4-bus distribution system

as per the proposal, can be mathematically expressed in equation 4.2,

$$I_{pickup} = I_{pre}^+ (1.1V^+) + 0.275 \quad (4.2)$$

where I_{pre}^+ is the pre-fault positive sequence current seen by the relay and input positive sequence voltage V^+ varies from 0 to 1 p.u. The fault resistance used in this project is 10 ohms. Also, the implemented VR-OCR works satisfactorily for faults at distant locations (100 km). The simulation and results are discussed in the next chapter

4.4 Summary

The protection of DER has been discussed in the above chapter. Two different types of relays have been used: one is Extremely Inverse OCR, and the other is voltage-restrained OCR. The latter is more effective because it considers both positive sequence fault voltage and current to trip the circuit. Also, voltage-restrained OCR works effectively with different loading conditions and at different fault locations.

Chapter 5

Simulation Results and Discussion

5.1 Introduction

To assess the functionality of the simulated solar PV model under low voltage ride-through (LVRT) conditions, a line-to-line ground (LLG) fault is induced at the point of coupling (POC) depicted in Figure 5.1, at 5 seconds.

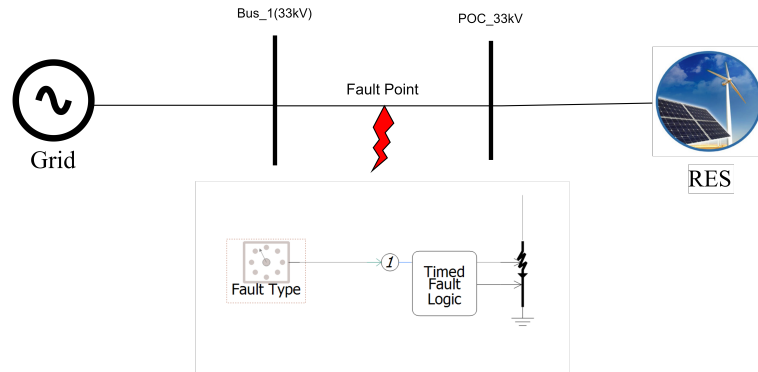


Figure 5.1: Fault at POC of SPV at 5 sec of time

From Figure 5.2, the PV plant root mean square (RMS) voltage is 1 pu before the contingency. During

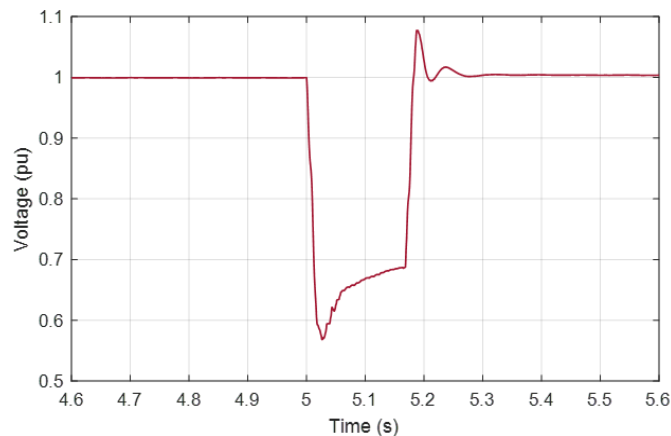


Figure 5.2: Voltage dip at POC bus in pu during fault

the inception of the fault at 5 sec, the voltage level drops to 0.67 pu and recovers to 1 pu after the removal of the fault at 5.667 sec. On sensing the voltage level falling below 0.8 pu, SPV satisfies the LVRT condition, taking the voltage and reactive power graph into consideration.

There is no reactive power (Q) supply before fault, only active power of 25 MW is supplied by SPV. But at the time of contingency, from Figure 5.3, it is observed that the SPV system remains connected to the system and supplies reactive power of above 12 MVar to support the bus voltage and then returns to its nominal value when the fault is cleared from the system. The reactive power is supplied into the grid integrated by the PV plant according to the severity of the fault. The active power (P), before the fault occurs, is at a nominal value and during the fault time graph line starts falling and rises back to a normal level as the fault is cleared. The nominal current is 0.435 pu. During the inception of fault, the PV current

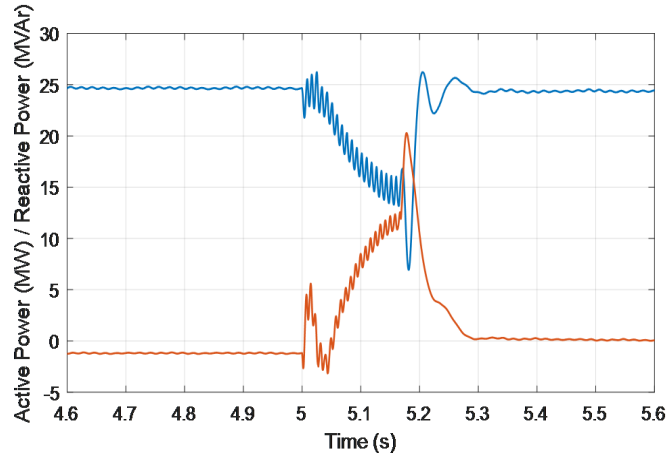


Figure 5.3: supply of reactive power in pu after the inception of fault

in the initial transient period can go beyond two times the rated current but the steady state fault current from SPV goes up to 1.5 times the rated current as can be observed from the graph shown in Figure 5.4. The current limit for preventing switches is set to 1.5 times the full load current. From the results, we

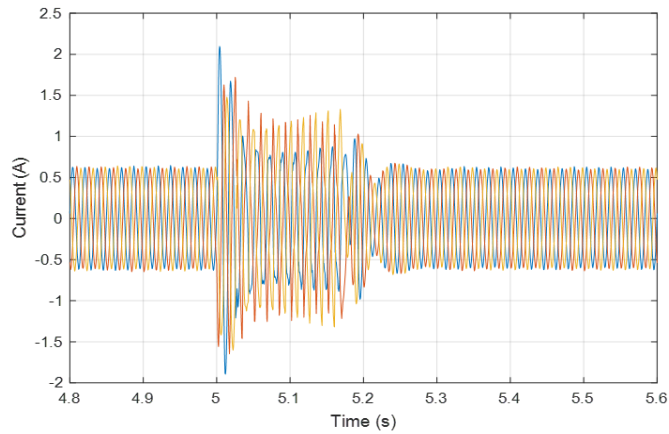


Figure 5.4: Fault current supplied by SPV in pu

can conclude that modelled solar PV adheres to the grid codes and satisfies LVRT conditions by remaining

connected to the grid during contingency and supplying reactive power to the PV bus.

From Figure 5.5, it can be observed that during symmetrical fault the positive sequence component is mainly present in the fault current as SPV always supplies a balanced current irrespective of the condition. The graph also uses the presence of these sequence elements to highlight how the short-circuit current (SCC)

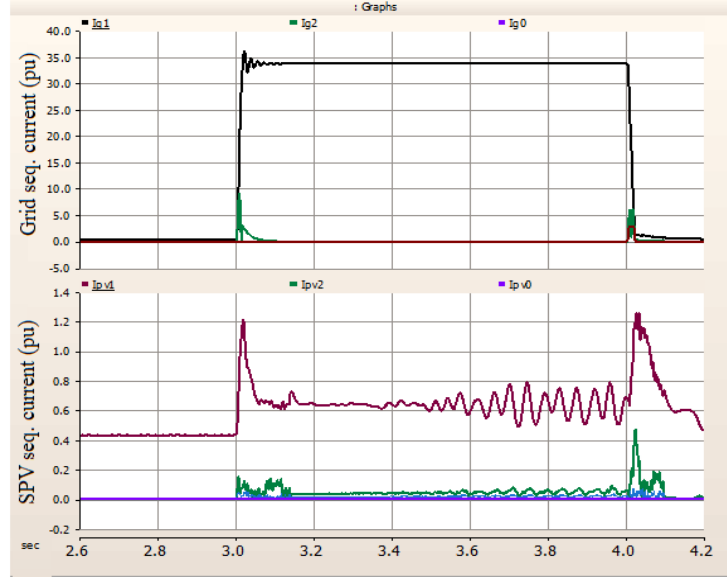


Figure 5.5: SCC in its sequence representation for a LLLG:(a) grid contribution and (b) PV inverter contribution

from the grid and the SCC from the PV inverter differ from one another. To illustrate the contribution of fault current during SLG and LLG faults, Figures 5.6 and 5.7 show the respective SSC contributions from the PV system and grid. It can be observed that during unsymmetrical fault positive sequence is the main

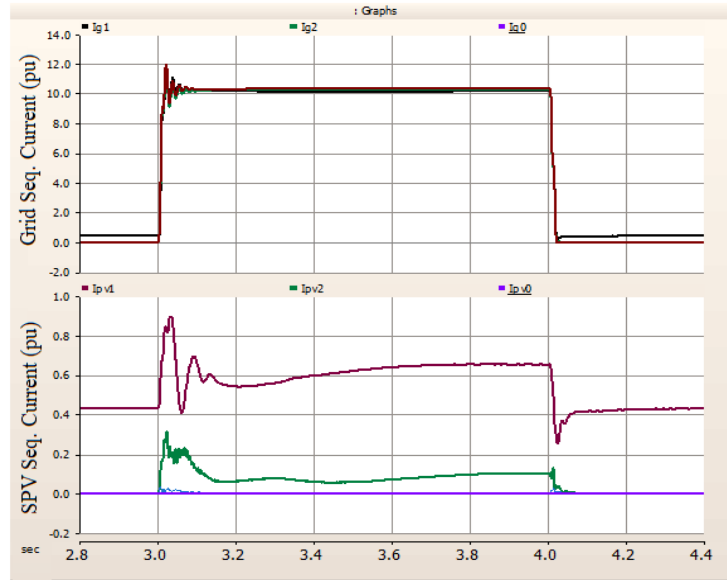


Figure 5.6: SCC in its sequence representation for an SLG: (a) grid contribution and (b) PV inverter contribution

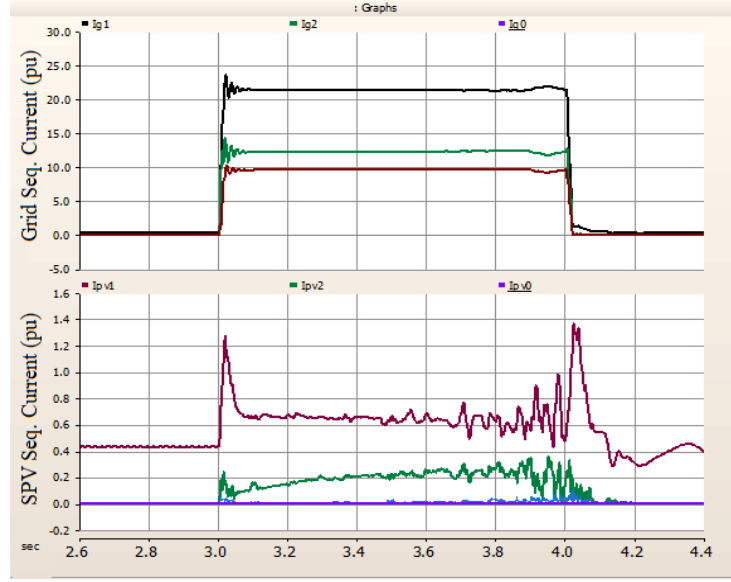


Figure 5.7: SCC in its sequence representation for an LLG fault event

component along with a small negative sequence component. This discussion concludes the importance of using the positive sequence component of current and voltage in designing voltage-restrained OCR.

5.2 Over-Current Fault Simulation results

A sustained fault is created at 3 seconds, and the fault current distribution from the PV system is observed. The power system under consideration is a simple 3-bus system illustrated in Figure 5.8. The

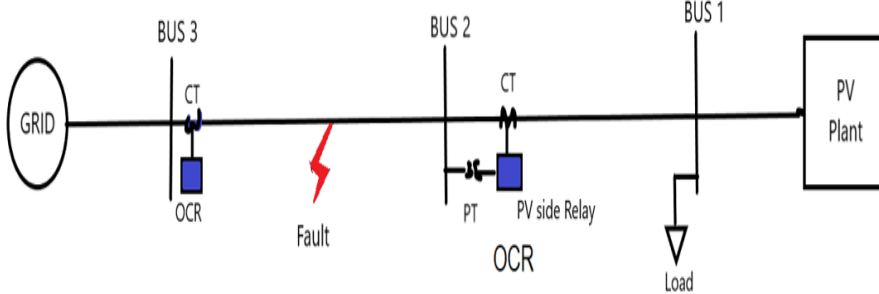


Figure 5.8: A PV plant integrated three-bus distribution system

simulation is observed for a high penetration level of 25 % with respect to the load and at two different fault levels:

5.2.1 Line to Ground fault

A line to ground fault is introduced between bus-1 and bus-2 of the mentioned 3-bus system. The fault current is analyzed through the graph plot of Figure 5.9 and it is observed that there is a very high rise in current(+ve sequence). The fault current is provided to OCR through the current transformer. The OCR settings detect the fault current higher than its pickup value and thus send a trip signal to the circuit

breaker. The circuit breaker opens the circuit.

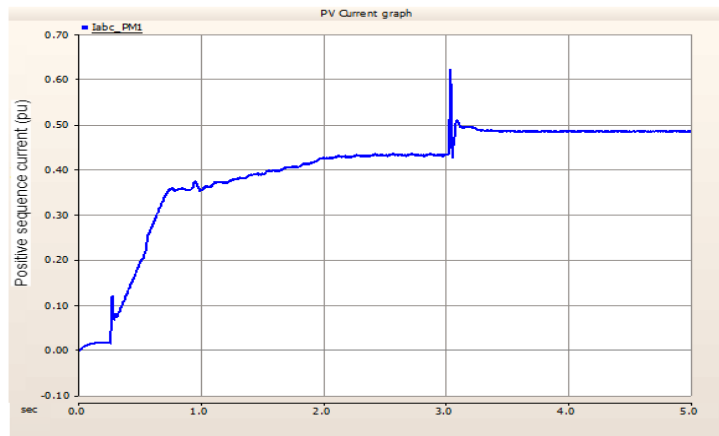


Figure 5.9: CT primary and secondary fault level and positive sequence current of LG fault

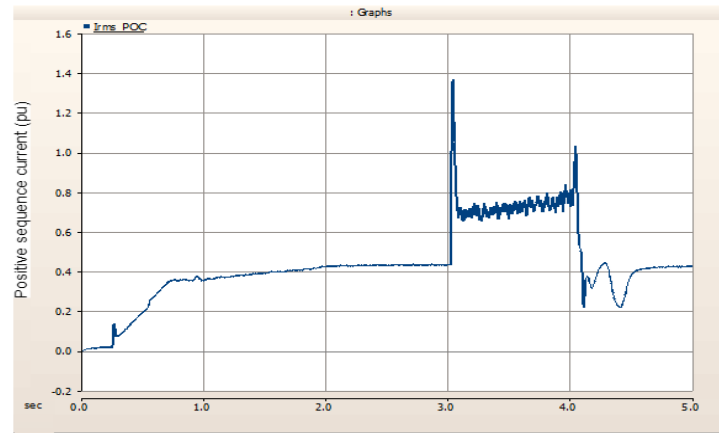


Figure 5.10: CT primary and secondary fault level and positive sequence current of LLL fault

5.2.2 Line to Line to Line fault

A triple line fault is created between bus 1 and bus 2 of mentioned 3-bus system. The fault current is seen through the graph-plot of Figure 5.10 and it is observed that there is a very high rise in current(+ive sequence) level. The fault current is fed to OCR. The OCR detects the fault current higher than its pickup value and thus sends a trip signal to the circuit breaker.

5.3 Voltage-Restrained Over-Current

Three types of faults are observed (LG, LLG, LLLG) on the given system as shown in Figure 5.11. The load on the system is varied from no load to 30 % of the loading condition.

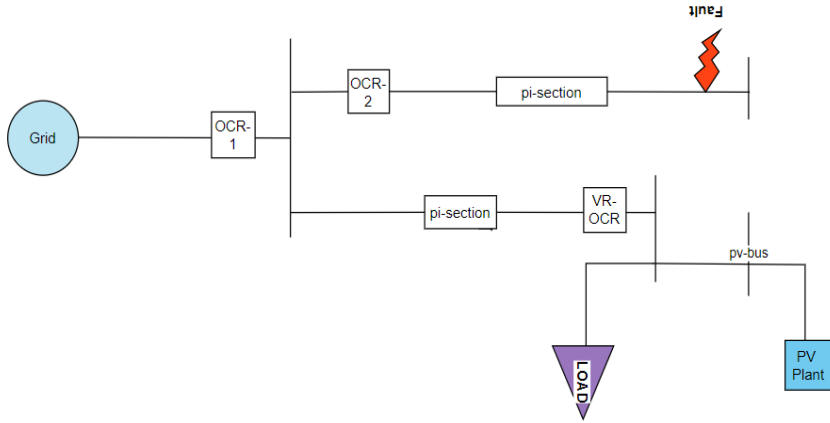


Figure 5.11: A PV plant integrated 4-bus distribution system

5.3.1 Line to Ground Fault

A line-to-ground (LG) fault was introduced at 4 seconds between bus1 and bus-2 of the mentioned 4-bus system. From Figure 5.12, it is observed that the root mean square (RMS) value of the nominal current is 0.95 pu and during the inception of fault current rises to 1.28 pu. similarly, from Figure 5.13, it is observed the nominal RMS voltage is 1 pu and during the contingency, the voltage level sags to 0.78 pu. As the pickup current follows the voltage, it falls from 1.15 pu to 0.86 pu as shown in Figure 5.14. Thus isolating the faulty section. The relay's pickup-voltage curve can be seen in Figure 5.21.

5.3.2 Line to Line to Ground Fault

A line-to-ground (LLG) fault was introduced at 4 seconds between bus1 and bus2 of the mentioned 4-bus system. From Figure 5.15, it is observed that the root mean square (RMS) value of the nominal current is 0.95 pu and during the inception of fault current rises to 1.4 pu. similarly, from Figure 5.16, it is observed the nominal RMS voltage is 1 pu and during the contingency, the voltage level sags to 0.544 pu. As the pickup current follows the voltage, it falls from 1.18 pu to 0.64 pu as shown in Figure 5.17. Thus isolating the faulty section. The relay's pickup-voltage curve can be seen in Figure 5.21.

5.3.3 Line to Line to Line to Ground Fault

A line-to-ground (LLLG) fault was introduced at 4 seconds between bus1 and bus-2 of the mentioned 4-bus system. From Figure 5.18, it is observed that the root mean square (RMS) value of the nominal current is 0.95 pu and during the inception of fault current rises to 4.2 pu. similarly, from Figure 5.19, it is observed the nominal RMS voltage is 1 pu and during the contingency, the voltage level sags to 0 pu. As the pickup current follows the voltage, it falls from 1.18 pu to 0.275 pu as shown in Figure 5.20. As the voltage level

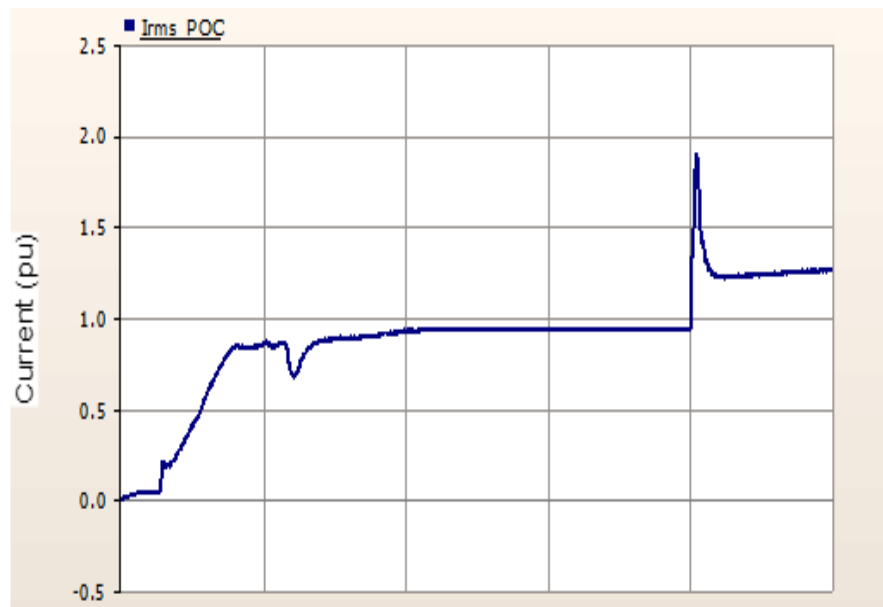


Figure 5.12: RMS current of LG fault

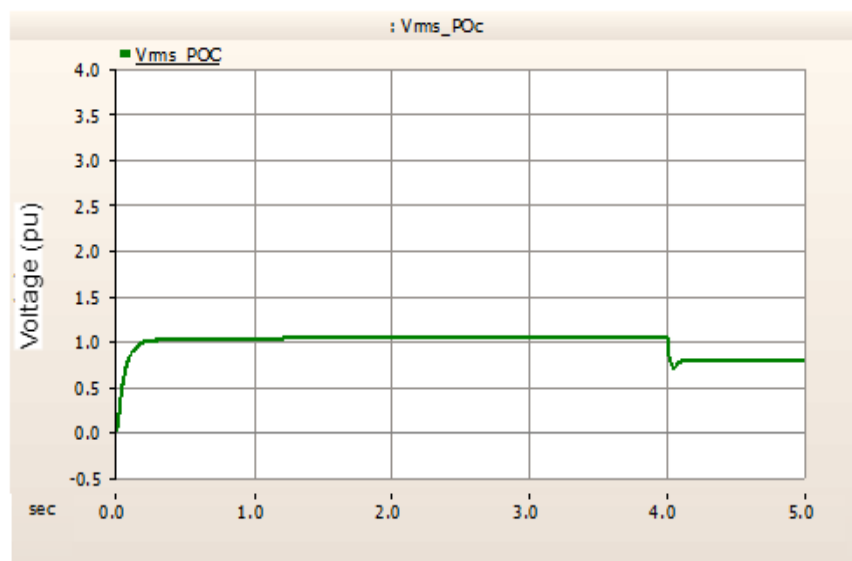


Figure 5.13: RMS voltage of LG fault

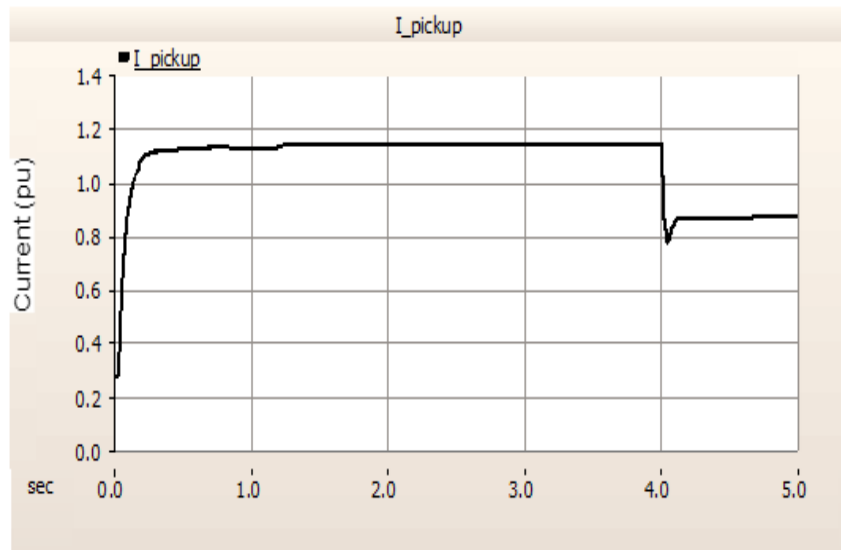


Figure 5.14: Pick-up current of LG fault

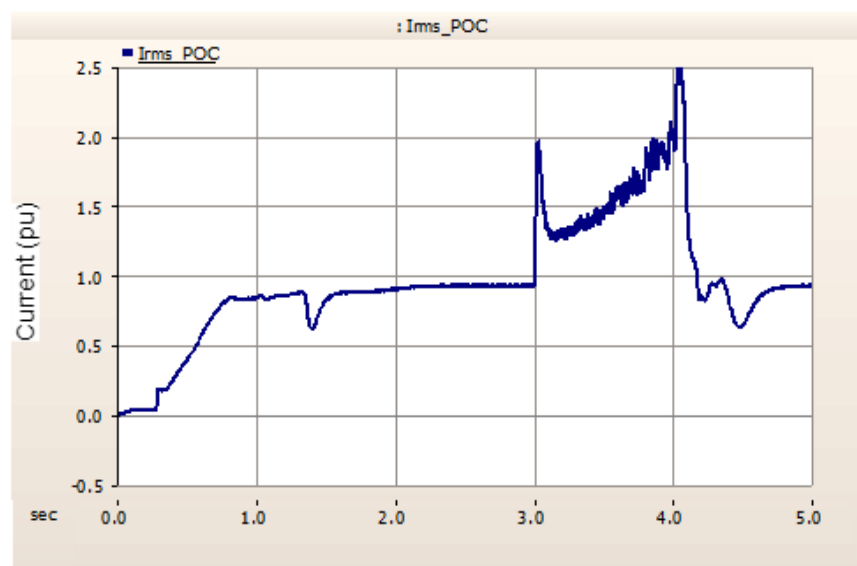


Figure 5.15: RMS current of LLG fault

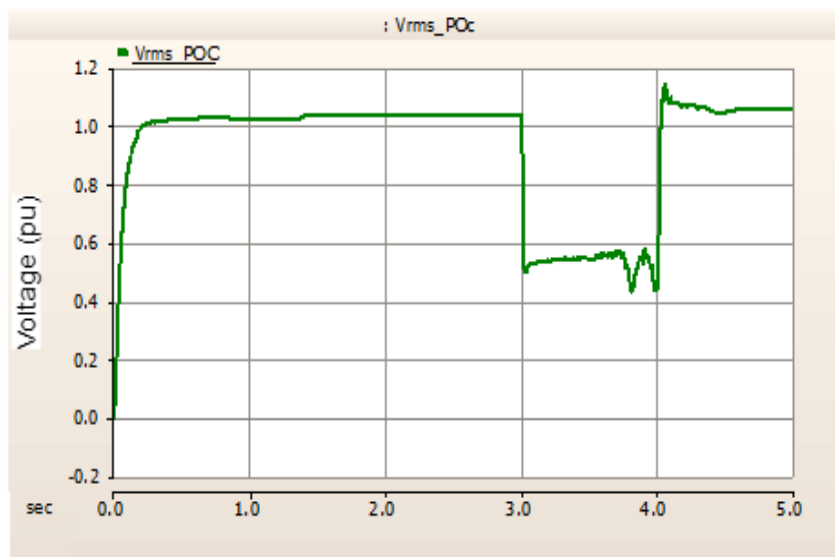


Figure 5.16: RMS voltage of LLG fault



Figure 5.17: Pick-up current of LLG fault

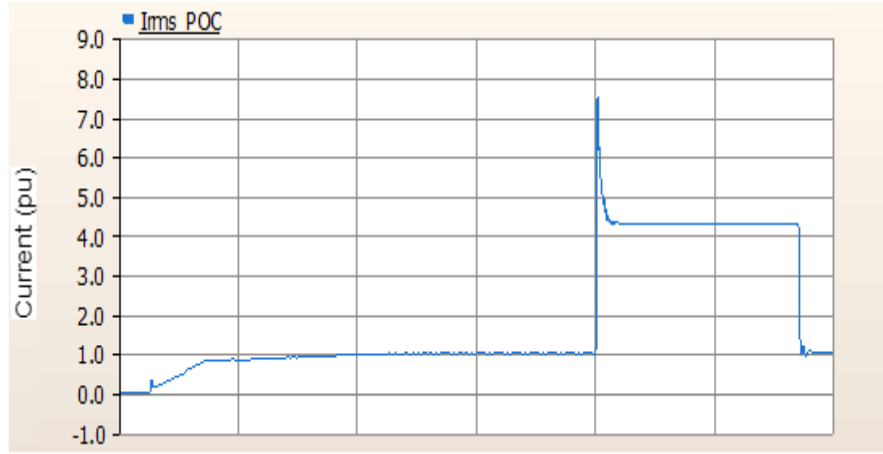


Figure 5.18: RMS current of LLLG fault

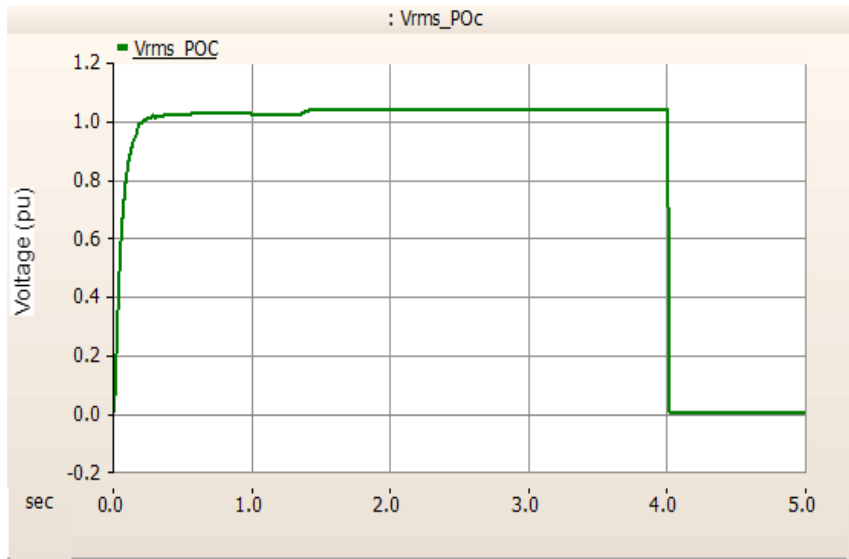


Figure 5.19: RMS voltage of LLLG fault

falls to 0 pu the current retains the minimum value of 0.275 pu. This isolates the faulty section. The relay's pickup-voltage curve can be seen in Figure 5.21. The graph shown in Figure 5.21 depicts the relationship between pick-up currents for respective voltage dips and fault types.

From the above observations, it is verified that the pickup current is modifying its value according to the voltage dip and is a function of both voltage and current. Thus VR-OCR is more versatile than conventional OCRs which take the magnitude of current only into consideration during fault detection. The relay functions properly for the mentioned loading condition. As the load is increased beyond 40 % the relay malfunctions as is discussed in the next section

5.4 VR-OCR with different loading conditions

In this section, the SPV is set to different loading percentages, namely fully loaded and half loaded. All three types of faults (LG, LLG, LLLG) that were created in the previous section are now introduced again

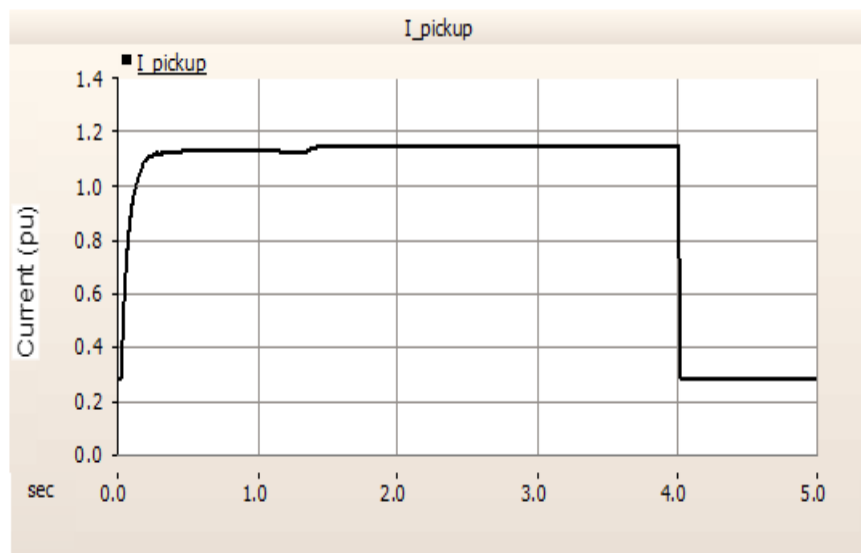


Figure 5.20: Pick-up current of LLLG fault

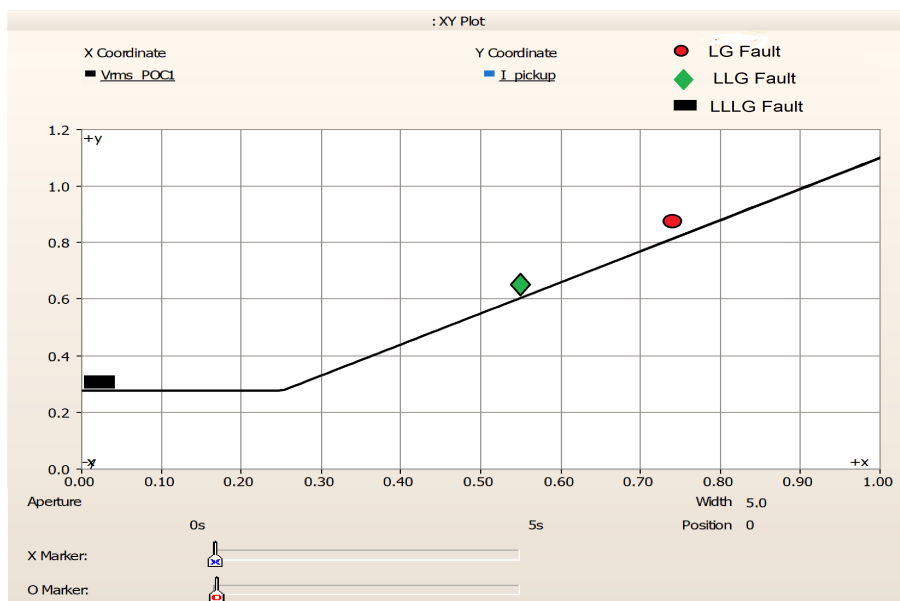


Figure 5.21: Voltage and current seen by relay for different faults

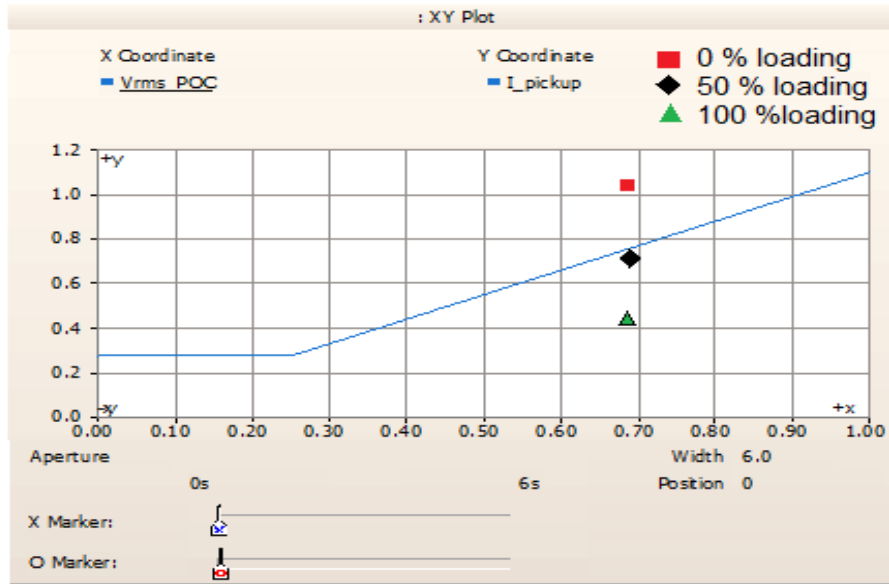


Figure 5.22: Voltage and current seen by VR-OCR during fault at 0%, 50% and 100% loading condition

with the given loading percentages

It is observed that the existing VR-OCR characteristics correctly identify the fault for the 0% loading condition. However, it fails to operate for an increase in the loading condition to 50% and 100%, as shown in Figure 5.22. The limited current supplied by the PV plant is to prevent the switches of the PV inverter from burning. As the loading increases, the fault current observed by the relay decreases as can be observed from Table 5.1. This leads to a relationship between voltage and current in the block zone. It indicates that the

Table 5.1: Comparison of fault current for different load percentage

Percentage Loading	Fault current contribution from PV
100 %	0.15 pu
50 %	0.22 pu
0 %	0.32 pu

performance of the existing VR-OCR for line protection is influenced by the pre-fault loading condition or pre-fault current observed by the relay. To address this issue, a modified pickup current value is developed based on the pre-fault current and bus voltage. This modified pickup current value ensures satisfactory tripping for different loading conditions, as discussed in Chapter 4. The PSCAD circuit diagram illustrating this is shown in Figure 5.23.

5.4.1 At 50% loading condition

A fault occurs between buses 1 and 2 within the mentioned 4-bus system. This system is exposed to all three types of faults, and it has been observed that the relay dynamically adjusts its pickup setting based on the pre-fault current. The successful operation of the relay for the specified load percentage is confirmed by referring to the graph depicted in Figure 5.24.

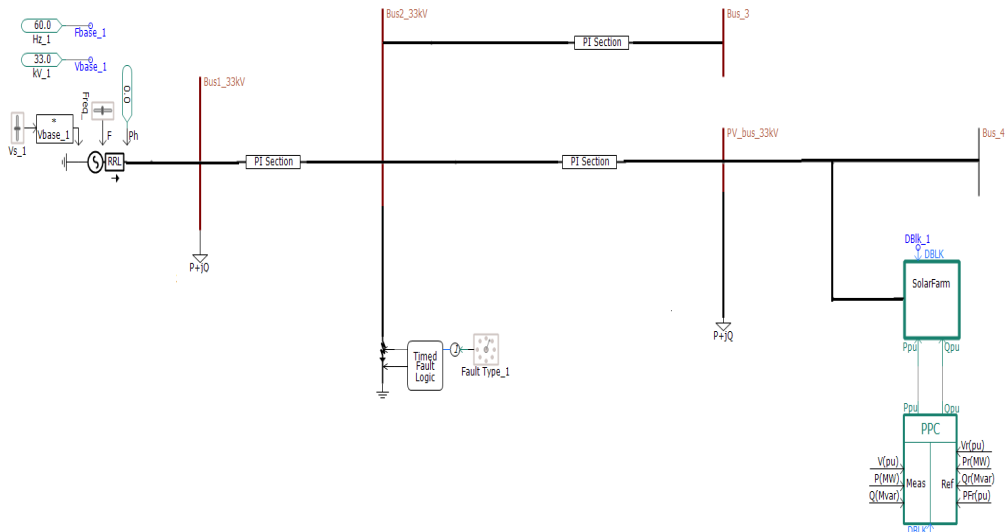


Figure 5.23: Schematic diagram of PV integrated 4-Bus system

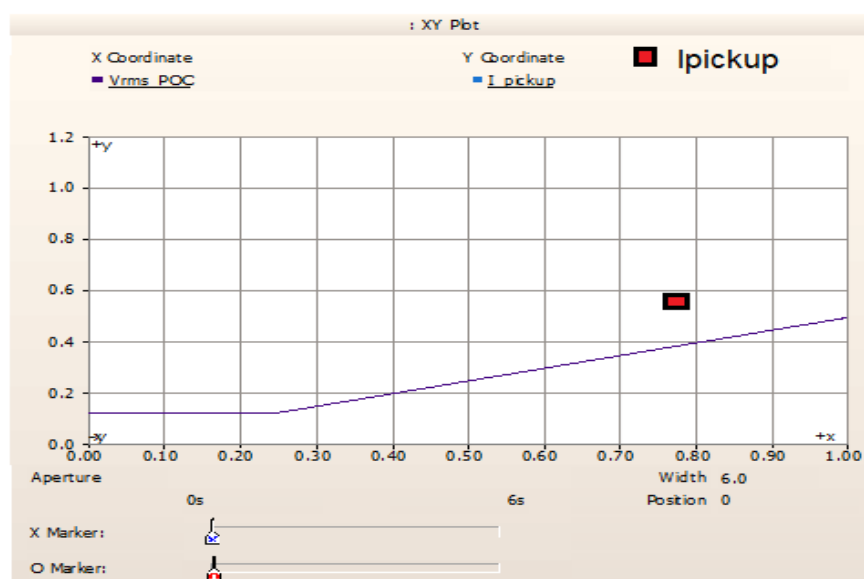


Figure 5.24: Proposed adaptive VR-OCR characteristics for 50% loading conditions at PV bus

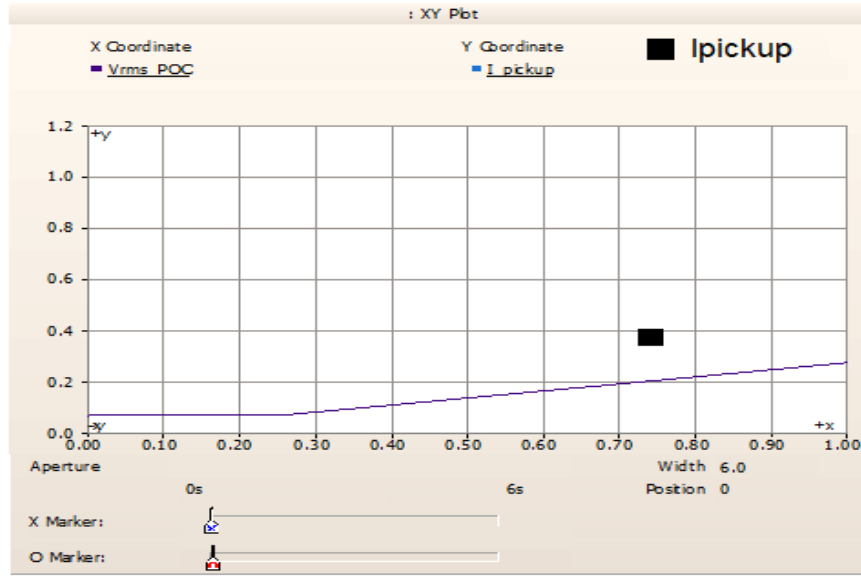


Figure 5.25: Proposed adaptive VR-OCR characteristics for 100% loading conditions at PV bus

5.4.2 At 100% loading condition

A fault is introduced between buses 1 and 2 within the mentioned 4-bus system. This system experiences all three types of faults, and it is noted that the relay dynamically adjusts its pickup setting based on the pre-fault current. By referring to the graph in Figure 5.25, it is confirmed that the relay effectively operates for the specified load percentage. The proposed setting updates the pickup characteristics with loading conditions

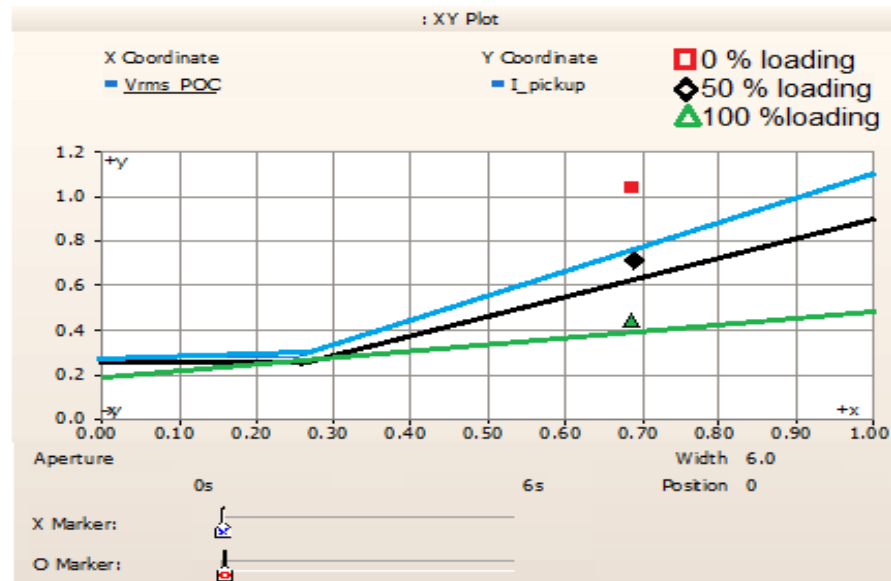


Figure 5.26: Existing and Proposed adaptive VR-OCR characteristics for different loading conditions at PV bus

and detects the fault correctly. It indicates that the adaptive pickup setting improves the performance of the relay in case of high-loading situations. Figure 5.26., cumulatively depicts the satisfactory operation of

adaptive voltage-restrained OCR for various loading conditions.

5.5 Summary

The fault current used in OCR is a positive sequence component of the current since the PV control strategy supplies balanced current during fault conditions. The voltage-restrained over-current relay is using the pre-fault current and fault voltage to trip the circuit breaker. The fault calculation is done for low-resistance faults (up to 10 ohms). The main focus of the work was to develop and implement adaptive VR-OCR which was done satisfactorily. The relay coordination between VR-OCR and overcurrent relays is the future work.

Chapter 6

Real Time validation of PV-Integrated Grid

6.1 Introduction

The integration of photovoltaic (PV) systems into the grid can be achieved using hardware implementation with Speedgoat and MATLAB. Speedgoat is a real-time target machine that enables rapid control prototyping and hardware-in-the-loop simulation. MATLAB, on the other hand, provides a comprehensive set of tools for modelling, simulation, and control design.

To implement a PV-integrated grid using Speedgoat and MATLAB, the first step is to model the PV system using the PV module characteristics, environmental conditions, and power converters. MATLAB offers tools like Simulink and Simscape Power Systems for building such models.

Next, the model can be deployed onto the Speedgoat real-time target machine. Speedgoat provides a robust and high-performance platform for executing real-time simulations. The PV system model is connected to the Speedgoat I/O modules, which interface with the hardware components such as PV inverters and grid interfaces.

6.2 Speedgoat Target Machine

Speedgoat implementation involves the seamless integration and utilization of Speedgoat real-time target machines in various engineering and scientific applications. Speedgoat, a renowned provider of high-performance real-time solutions, offers hardware platforms specifically designed for rapid control prototyping, hardware-in-the-loop (HIL) testing, and real-time simulation.

The implementation process begins with configuring the Speedgoat target machine to meet the specific requirements of the application. This includes selecting the appropriate model and capacity and configuring the I/O interfaces to interface with external systems and devices.

Once configured, we can leverage popular software tools like MATLAB, Simulink, and LabVIEW to develop and deploy real-time control algorithms or models directly on the Speedgoat target machine. This enables rapid iteration, validation, and evaluation of control strategies in a real-time environment.

Speedgoat can interface with external systems such as sensors, actuators, and other devices, facilitating comprehensive hardware-in-the-loop (HIL) testing. This allows us to validate designs, evaluate system behaviour,

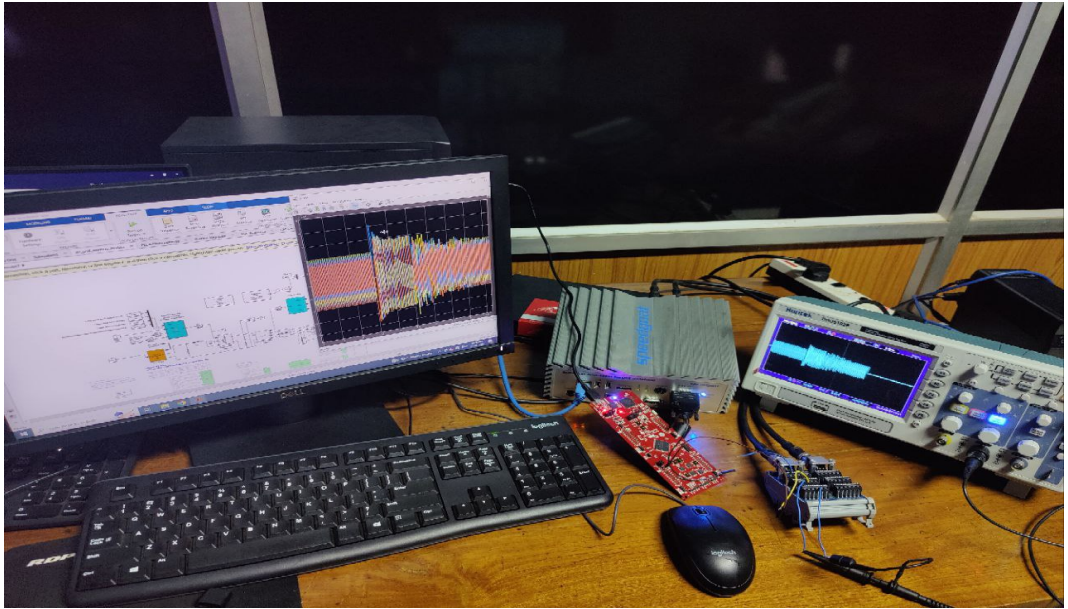


Figure 6.1: Speedgoat hardware module

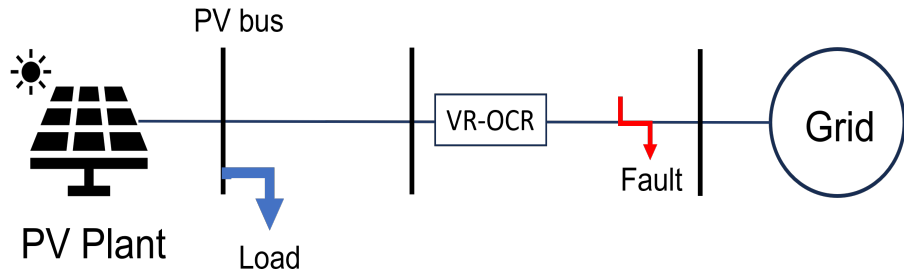


Figure 6.2: MATLAB 3-bus model

and perform real-time testing with realistic hardware interactions. The speedgoat module is shown in Figure 6.1.

6.3 Implementation of PV-integrated grid into Speedgoat Target Machine

The implementation of a photovoltaic (PV)-integrated grid into Speedgoat using MATLAB involves integrating PV system models and control algorithms into the Speedgoat real-time target machine for real-time simulation and testing.

6.3.1 MATLAB model with voltage restrained OCR

To begin, we have created a PV system model using MATLAB/Simulink. This model would include components such as PV panels, DC-DC converters, inverters, and grid connections. The model should accurately represent the behaviour and characteristics of the PV system.

A 3-bus PV-integrated gird system is created in MATLAB. The system is made to run before being deployed on the target machine. The SPV integrated grid system and developed voltage-restrained OCR that has been developed in PSCAD are created here because we are going to implement the same system in hardware

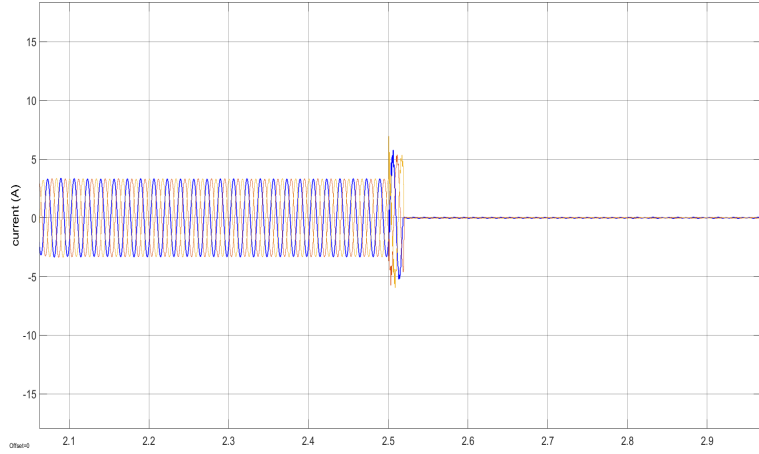


Figure 6.3: Fault current after the opening of circuit breaker

speedgoat for validation. In Figure 6.2, the fault is created between buses 1 and 2 of the PV integrated grid system. From Figure 6.3, it is observed that the PV integrated grid system in MATLAB, when put into fault condition, the voltage-restrained OCR trips the circuit breaker and isolates the faulty system as per desired results.

6.3.2 Real Time implementation

Speedgoat offers a range of modules(IO191, IO397, IO594 etc) designed for various applications. In this work, we have used speedgoat module IO191. IO191 is a specific I/O module offered by Speedgoat, known as the IO191-S100. The IO191 module is designed to provide high-speed and accurate analog and digital I/O capabilities for real-time applications.

The IO191 module features a variety of input and output channels, including 16 analog inputs, 4 analog outputs, 16 digital inputs, and 16 digital outputs. The analog inputs support a wide voltage range with high-resolution ADCs, allowing for precise measurements of analog signals. The analog outputs provide voltage or current signals for controlling external devices. To configure the IO191 Speedgoat module for a PV-integrated grid system and specify voltage levels, we will be following the below-mentioned steps:

Hardware Setup: Ensure that the IO191 Speedgoat module is properly connected to your computer. Connect the necessary cables to interface with the PV system, such as communication cables, power cables, and voltage measurement connections. **Software Setup:** Install the required software and drivers provided by Speedgoat for the IO191 module. Connect the IO191 module to your computer using the appropriate connection method (e.g., Ethernet, USB). Ensure that your computer has the necessary software tools, such as MATLAB/Simulink or a compatible real-time environment, to communicate with the IO191 module. The software tool such as MATLAB we are using should be of the same version as that installed in the Target machine. **Configuration:** Open the software environment (e.g., MATLAB/Simulink) and create a new project or model. Add the IO191 Speedgoat module to your model using the provided libraries. Configure the IO191 module parameters based on your PV integrated grid system requirements, including voltage level

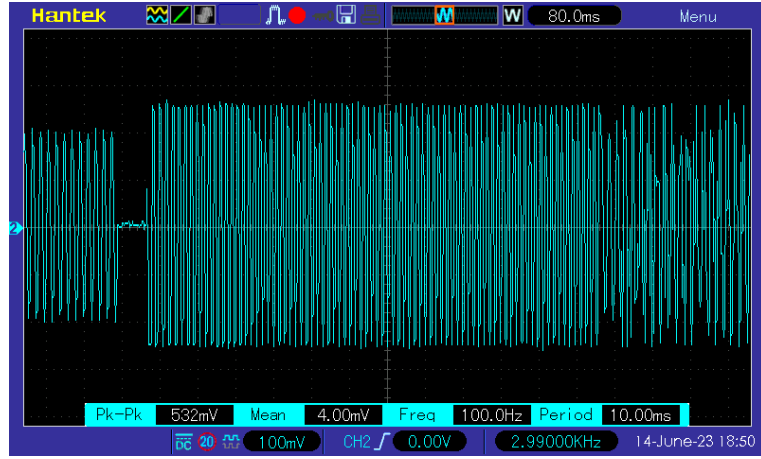


Figure 6.4: Open circuit voltage during fault



Figure 6.5: Open circuit voltage during fault

specifications, our voltage level is set to 5V. Now the voltage signals that we are feeding to the target machine are passed through a gain block first so that the voltage signal is in the same range as specified for the target machine (5V).

In the IO191 output analog module, we have selected channel 9 and ground. These voltage signals that actually show the opening of the circuit breaker are fed to a digital storage oscilloscope (DSO) to validate the same. From Figure 6.4 and Figure 6.5 shows the open circuit voltage and short circuit current respectively after the opening of the circuit breaker, observed through DSO.

6.4 Summary

The chapter discusses the integration of photovoltaic (PV) systems into the grid using hardware implementation with Speedgoat and MATLAB. Speedgoat is a real-time target machine used for control prototyping and hardware-in-the-loop simulation, while MATLAB provides tools for modelling, simulation, and control design. The process involves modelling the PV system using MATLAB tools like Simulink and Simscape Power Systems, deploying the model onto the Speedgoat real-time target machine, and connecting it to hardware components. Speedgoat allows for seamless integration and utilization in various applications,

offering high-performance platforms for real-time simulation and testing. The text also explains the configuration of the Speedgoat target machine and the IO191 module, which provides analog and digital I/O capabilities. The voltage signals are validated using a digital storage oscilloscope (DSO).

Chapter 7

Conclusion and Future Work

7.1 Conclusion

In grid-integrated PV systems, the contribution of fault current from the PV plant is significantly lower compared to conventional grid systems. This is primarily due to the thermally limiting nature of inverter switches, which restricts the amount of fault current that can be injected into the grid. However, in this study, it is demonstrated that the existing overcurrent relay (OCR) method, which relies on phase current, performs poorly during fault conditions in PV-integrated systems.

To address this issue, this project author proposes a new method for protecting the distribution system, which takes into account the local positive sequence current and voltage as inputs. The pickup current of the adaptive voltage-restrained OCR (VR-OCR) is determined as a function of positive sequence voltage and pre-fault conditions for all types of faults and varying load conditions. It is crucial to consider the load condition in PV-integrated grid systems which affects the pre-fault current seen by the relay.

The proposed method proves to be more advantageous compared to the existing OCR method. Incorporating the positive sequence current and voltage, along with pre-fault conditions. Thus provides a more accurate and reliable fault detection and protection mechanism. This approach takes into consideration the specific characteristics and limitations of PV systems, ensuring enhanced system performance and grid stability.

In conclusion, the study highlights the importance of utilizing alternative protection methods in PV-integrated grid systems. By considering local positive sequence current and voltage, the proposed method offers a more effective solution for fault detection and protection, overcoming the limitations of the conventional OCR approach.

7.2 Future Work

The project can be carried out with other renewable energy resources such as wind farms, batteries etc. The following points highlight the future work of the current project

- To develop an adaptive coordination scheme among protection elements during fault for a highly renewable penetrated system.
- To develop coordination between VR-OCR and OCRs of the system.
- To add a directionality element to the VR-OCR.

APPENDIX

The data are for 33kV, 60Hz power system:

PV module specifications.

Maximum Power = 25 MW

Open circuit Voltage = 1.015 kV

Short Circuit Current = 0.325 kA

Irradiation = 1000 W/m²

Temperature = 28°C

Number of series modules = 35

Number of Parallel modules = 130

Number of Units = 100

Publications

Owais Manzoor Malla, Athul Jose p and Deepak M, "Adaptive Over current protection of SPV Integrated Distribution Systems", 3rd International Conference on Power Electronics, Smart Grid, and Renewable Energy (PESGRE 2023)[Submitted].

Adaptive Over Current Protection of SPV Integrated Distribution Systems

Owais Manzoor Malla

Department of Electrical Engineering
National Institute of Technology
Calicut, India
owaismanzoor68@gmail.com

Athul Jose P

Department of Electrical Engineering
National Institute of Technology
Calicut, India
athulpulikkottil@gmail.com

Deepak M

Department of Electrical Engineering
National Institute of Technology
Calicut, India
deepakm@nitc.ac.in

Abstract—As the integration of solar photovoltaic (SPV) with traditional grid systems increases, various protection issues in distribution systems arise because of modified network topologies, limited fault current contribution, and bidirectional power flow. The low fault current contribution of inverter-based resources due to the thermal constraints of inverter switches causes the malfunction of the conventional over-current relay in the distribution system. Also, the varying load levels limit the work of conventional voltage-restrained relays. In this paper, a new procedure is developed to mitigate the issues with existing over-current relays (OCRs). This approach uses local positive sequence current and voltage values to modify the pickup current of the proposed relay operation and makes it adaptive for different loading conditions. SPV plants can operate in different modes of operation, such as voltage control, fixed reactive power control, and power factor control. In this paper, the SPV plant is operated in voltage control mode. In the voltage control mode of operation, the SPV plant complies with grid codes, i.e., follows the fault ride-through(FRT) condition. The method is developed and validated with PSCAD on an IEEE 9-bus system.

Index Terms—Distribution Energy Resources (DERs), Fault Ride Through (FRT), Over-Current Relay (OCR), Positive Sequence Component, Reactive Power, and Solar Photo Voltaic (SPV).

protection is mainly carried out through over-current relays (OCR) [5]. The OCR elements are programmed with multiple pickup configurations and operate based on the intensity of the current [6].

Detecting faults in inverter-based resources (IBRs) poses challenges for conventional overcurrent relays due to their reliance on the current magnitude as the primary criterion. This difficulty arises from the limited current rating of inverter switches, which makes fault detection more challenging. In traditional power networks, the synchronous machine, characterised by its significant rotor inertia and induction phenomenon, nature of network plays a predominant role in generating the fault current, which leads to a substantial and readily detectable fault currents for OCR [7]. Furthermore, the flow of power in the distribution system remains no more radial with renewable power plants, and the contribution of fault current from the main grid is reduced in magnitude after the point of common coupling (POC), causing blinding of protection [8]. One significant protection challenge faced by IBRs is the loss of relay coordination due to bidirectional

REFERENCES

- [1] Maity, Shibdas, et al. "Pollution tolerance performance index for plant species using geospatial technology: evidence from Kolaghat Thermal Plant area, West Bengal, India." *Spatial Information Research* 25 (2017): 57-66.
- [2] Bogdanov, Dmitrii, et al. "Low-cost renewable electricity as the key driver of the global energy transition towards sustainability." *Energy* 227 (2021): 120467.
- [3] Denholm, Paul, and Maureen Hand. "Grid flexibility and storage required to achieve very high penetration of variable renewable electricity." *Energy Policy* 39.3 (2011): 1817-1830.
- [4] Basak, Prasenjit, et al. "A literature review on integration of distributed energy resources in the perspective of control, protection and stability of microgrid." *Renewable and Sustainable Energy Reviews* 16.8 (2012): 5545-5556.
- [5] N. Nimpitiwan, G. T. Heydt, R. Ayyanar, and S. Suryanarayanan, "Fault current contribution from the synchronous machine and inverter-based distributed generators," *IEEE Transactions on power delivery*, vol. 22, no. 1, pp. 634–641, 2006.
- [6] Ojaghi, Mansour, and Vahid Mohammadi. "Use of clustering to reduce the number of different setting groups for adaptive coordination of overcurrent relays." *IEEE Transactions on Power Delivery* 33.3 (2017): 1204-1212.
- [7] Varma, Rajiv K. *Smart solar PV inverters with advanced grid support functionalities*. John Wiley Sons, 2021.
- [8] B. Ram, *Power system protection and switchgear*. Tata McGraw-Hill Education, 2011.
- [9] Han, Zhiqi. *Protection coordination in networks with renewable energy sources*. Diss. The University of Manchester (United Kingdom), 2014.
- [10] S. H. Horowitz, A. G. Phadke, and C. F. Henville, *Power system relaying*. John Wiley and Sons, 2022.
- [11] Denholm, Paul, and Robert M. Margolis. "Evaluating the limits of solar photovoltaics (PV) in traditional electric power systems." *Energy policy* 35.5 (2007): 2852-2861.

- [12] M. Meskin, A. Domijan, and I. Grinberg, "Impact of distributed generation on the protection systems of distribution networks: analysis and remedies—review paper," *IET Generation, Transmission and Distribution*, vol. 14, no. 24, pp. 5944–5960, 2020
- [13] Buraimoh, Elutunji, and Innocent E. Davidson. "Overview of fault ride-through requirements for photovoltaic grid integration, design and grid code compliance." *2020 9th International Conference on Renewable Energy Research and Application (ICRERA)*. IEEE, 2020.
- [14] Yazdani, A. (2018). *Modern Distribution Systems with PSCAD Analysis* (1st ed.). CRC Press.
- [15] Griffin, C. H., and J. W. Pope. "Generator ground fault protection using overcurrent, overvoltage, and undervoltage relays." *IEEE Transactions on Power Apparatus and Systems* 12 (1982): 4490-4501.
- [16] Haddadi, Aboutaleb, et al. "Impact of inverter-based resources on negative sequence quantities-based protection elements." *IEEE Transactions on Power Delivery* 36.1 (2020): 289-298.
- [17] Reno, Matthew J., et al. "Influence of inverter-based resources on microgrid protection: Part 1: Microgrids in radial distribution systems." *IEEE Power and Energy Magazine* 19.3 (2021): 36-46.
- [18] Tiwari, Ashutosh Kumar, Soumya Ranjan Mohanty, and Ravindra Kumar Singh. "Review on protection issues with penetration of distributed generation in distribution system." *2014 International Electrical Engineering Congress (iEECON)*. IEEE, 2014.
- [19] Yazdani, A. (2018). *Modern Distribution Systems with PSCAD Analysis* (1st ed.). CRC Press.
<https://doi.org/10.1201/9781315301518>
- [20] El Moursi, Mohamed Shawky, Weidong Xiao, and Jim L. Kirtley Jr. "Fault ride through capability for grid interfacing large scale PV power plants." *IET Generation, Transmission Distribution* 7.9 (2013): 1027-1036.
- [21] Telukunta, Vishnuvardhan, et al. "Protection challenges under bulk penetration of renewable energy resources in power systems: A review." *CSEE journal of power and energy systems* 3.4 (2017): 365-379.
- [22] J. Keller and B. Kroposki, "Understanding fault characteristics of inverter-based distributed energy resources," tech. rep., National Renewable Energy Lab.(NREL), Golden, CO (United States), 2010